

# Studying speed-accuracy trade-offs in best-of-n collective decision-making through heterogeneous mean-field modelling

Andreagiovanni Reina\*

*Institute for Interdisciplinary Studies on Artificial Intelligence (IRIDIA),  
Université Libre de Bruxelles, Brussels, Belgium*

Thierry Njougou, Elio Tuci, and Timoteo Carletti\*

*Department of mathematics and Namur Institute for Complex Systems, naXys  
University of Namur, Rue Grafé 2, B5000 Namur, Belgium*

\* *andreagiovanni.reina@gmail.com; timoteo.carletti@unamur.be*

To succeed in their objectives, groups of individuals must be able to make quick and accurate collective decisions on the best among alternatives with different qualities. Group-living animals aim to do that all the time. Plants and fungi are thought to do so too. Swarms of autonomous robots can also be programmed to make best-of-n decisions for solving tasks collaboratively. Ultimately, humans critically need it and so many times they should be better at it! Despite their simplicity, mathematical tractability made models like the voter model (VM) and the local majority rule model (MR) useful to describe in simple terms such collective decision-making processes. To reach a consensus, individuals change their opinion by interacting with neighbours in their social network. At least among animals and robots, options with a better quality are exchanged more often and therefore spread faster than lower-quality options, leading to the collective selection of the best option. With our work, we study the impact of individuals making errors in pooling others' opinions caused, for example, to reduce the cognitive load. Our analysis is grounded on the introduction of a model that generalises the two existing VM and MR models, showing a speed-accuracy trade-off regulated by the cognitive effort of individuals. We also investigate the impact of the interaction network topology on the collective dynamics. To do so, we extend our model and, by using the heterogeneous mean-field approach, we show that another speed-accuracy trade-off is regulated by network connectivity. An interesting result is that reduced network connectivity corresponds to an increase in collective decision accuracy.

## I. INTRODUCTION

Reaching a consensus in a group of individuals without any central authority or coordinator requires individuals to exchange opinions and combine conflicting information received from peers. Studying the situation in which the group must agree on the best among a set of options, the so-called best-of-n problem, is interesting because it helps us to both understand biological processes and design the robotics systems of our future [1, 2]. Social insects are an example of collectives which need to solve the best-of-n problem when selecting the site where to nidificate [3–5]. While each insect makes an inaccurate estimate of the quality of each site, the colony is able to filter noise and reach a consensus on the best alternative [6]. Similarly, other more complex animals make collective decisions on the moment and direction to flee danger or the location where to forage [7–9]. Collective agreement is achieved by individuals sharing their opinion with others (voting) and, in turn, adopting the opinion expressed by others' votes. These simple voting rules employed by animals are an useful source of inspiration to design algorithms of robot swarms, which make best-of-n decisions, for example, on the shortest path to navigate [10, 11] or the most important location for their operations [12, 13].

The group is able to select the best alternative because each individual shares her opinion as frequently as the estimated quality, that is, better alternatives are shared

(voted) more often [14, 15]. Despite the individual estimates being incorrect, the collective dynamics led to a consensus for the option that, on average, is estimated of higher quality. Depending on the effort individuals make in acquiring, processing, and sharing information in their social network, the collective dynamics change, e.g., in the group accuracy or the decision speed. While there are several studies analysing voting models in decentralised networks [16–19], there is no explicit connection between the individual cognitive requirements, the social network, and the collective decision-making performance.

Here, we build a model that explicitly considers the cognitive effort that individuals make in acquiring and processing their neighbour's vote. The more cognitive effort individuals put in, the better they pool social information (making smaller pooling errors). We investigate how speed and accuracy change in collective decisions both as a function of the individual cognitive load and the interaction network. Our analysis reveals that an increased cognitive effort leads to quicker and more democratic collective decisions which however are not necessarily accurate. Counter-intuitively, the highest levels of collective decision accuracy can be achieved with moderate levels of cognitive efforts, however, at the expense of longer deliberation time. Thus, our model enriches our understanding of the classical speed-accuracy trade-off in decision-making [13, 20–23] by describing it through the

lens of individual cognitive load.

Additionally, our network analysis reveals that groups that are sparsely connected can obtain higher collective accuracy than when they are highly connected. Recent previous research has shown that in a number of conditions, having reduced connectivity between the group members can improve collective performance in terms of coordination, accuracy, or response speed [24–29]. More precisely, fish adaptively change their interaction network when exposed to a threat in order to maximise information transfer in the fish school [25]. Robots that can only run simplistic algorithms can also exploit the advantages of sparse connections to improve swarm accuracy [28, 30]. While it is commonplace to assume that higher connectivity can improve opinion sharing and thus lead to better coordination, these recent results show in which conditions limited connectivity can lead to improved collective dynamics. Our analysis uses the Heterogeneous Mean-Field theory (HMF) [31–34] to show that both network connectivity and individual cognitive load can be control parameters to regulate the speed-accuracy trade-off of group decision-making.

## II. THE MODEL

Let us consider a population composed of  $N$  agents making a binary collective decision between two alternative options, say  $A$  and  $B$ . Each option is characterised by a quality,  $Q_A$  and  $Q_B$  (for option  $A$  and  $B$ , respectively); without lack of generality we hereby assume  $Q_A > Q_B > 0$  and we will define the quality ratio  $Q = Q_B/Q_A \in (0, 1)$ . Each agent, at a given time  $t$ , has an opinion in favour of either option,  $A$  or  $B$ . Throughout the collective decision-making process, agents interact with each other and change their opinions depending on the votes expressed by their neighbours. Each agent votes with a frequency linearly proportional to the estimated quality of each option, thus  $Q_A$  and  $Q_B$  for options  $A$  and  $B$ , respectively. Therefore, through mean-field approximation, we model the change of agents' opinions as a function of the number of agents with opinion  $A$  and  $B$ , denoted by  $n_A(t)$  and  $n_B(t)$ , respectively, weighted by the respective option's quality and normalised by the group size  $N$ . Such weighted proportions,  $n_A^\#$  and  $n_B^\#$ , represent the mean-field approximation of the votes expressed by the agents in favour of option  $A$  and  $B$ , respectively, and correspond to

$$\begin{aligned} n_A^\# &= \frac{Q_A n_A / N}{Q_A n_A / N + Q_B n_B / N} \quad \text{and} \\ n_B^\# &= \frac{Q_B n_B / N}{Q_A n_A / N + Q_B n_B / N}. \end{aligned} \quad (1)$$

Agents can put different levels of effort into acquiring others' votes and processing them; we name such levels of effort as the agents' cognitive load in making their collective decisions. Different levels of cognitive load lead

to different levels of error in pooling social information. Numerous previous studies have considered agents with a low cognitive load, in the form of the *voter model* (VM) [17, 35–40], and with high cognitive load, in the form of the *majority rule model* (MR) [41–44]. In the VM, an agent samples a single vote, taken from a random agent, and adopts her opinion; therefore the probability that an agent committed to  $A$  changes her opinion to  $B$  is equal to the weighted proportion  $n_B^\#$ . Instead, in the MR, an agent has a higher cognitive load and she samples all votes received from the other agents and selects the most-voted option. In the majority rule model, agents do not commit pooling errors, whereas in the voter model, agents introduce a higher pooling error by sampling a single random vote. We build a model that generalises the two existing models and can also interpolate, in a continuous way, the cognitive load level in the form of pooling error among the two models and beyond. In our model, agents change their opinion with probability

$$P_\alpha(x) = \begin{cases} \frac{1}{2} - \frac{1}{2}(1-2x)^\alpha & \text{if } 0 \leq x \leq \frac{1}{2} \\ \frac{1}{2} + \frac{1}{2}(2x-1)^\alpha & \text{if } \frac{1}{2} < x \leq 1, \end{cases} \quad (2)$$

where  $x$  is the weighted proportion of agents with a different opinion. Therefore, an agent with an opinion in favour of option  $A$  (resp.  $B$ ) will change her opinion to  $B$  (resp.  $A$ ) with probability  $P_\alpha(n_B^\#)$  (resp.  $P_\alpha(n_A^\#)$ ). Note that the assumption of fixed population,  $n_A(t) + n_B(t) = N$ , implies  $n_A^\#(t) + n_B^\#(t) = 1$  and therefore, as a consequence of the functional form of Eq. (2), we have

$$P(n_A^\#) + P(n_B^\#) = 1. \quad (3)$$

The parameter  $\alpha \geq 0$  of Eq. (2) is the pooling error which allows controlling agents' cognitive load. For  $\alpha = 0$ , the model corresponds to the MR; for  $\alpha = 1$  to the VM.

Fig. 1 shows a graphical representation of  $P_\alpha(x)$  of Eq. (2) and let us appreciate that intermediate values of the pooling error  $\alpha$  allow interpolating between the two models. Indeed, values of  $0 < \alpha < 1$  represent cases in which an agent makes a higher effort than sampling a random individual (as she does in the voter model), still the probability of changing opinion in favour of the most-voted option is lower than the 'perfect' case (zero error) of the majority rule model. These intermediate values represent conditions in which the agent samples only a subset of the population or approximately and imprecisely integrates others' votes. Values of  $\alpha > 1$  further reduce the cognitive effort that the agent puts into taking into consideration others' opinions. As the value of the pooling error  $\alpha$  increases, the probability  $P_\alpha(x)$  gradually becomes more and more independent of the actual votes. For  $\alpha \gg 1$ , the probability of changing opinion approximates the flat line  $P_\alpha(x) = 0.5$ , that is, the agents make maximum levels of pooling error by randomly changing their opinion regardless of the opinions expressed by the others.

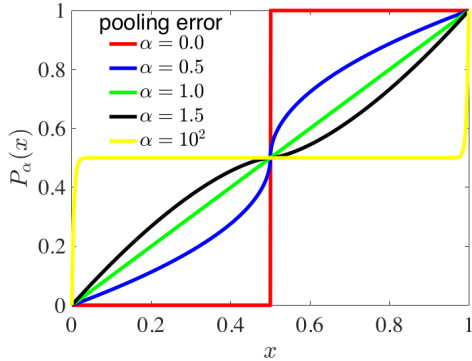


FIG. 1. The probability  $P_\alpha(x)$  given by Eq. (2) for representative values of the pooling error  $\alpha$ , which is a parameter inversely proportional to agents' cognitive load. For  $\alpha = 0$ , our model corresponds to the majority rule model [42], for  $\alpha = 1$  our model corresponds to the voter model [35, 36], for  $0 < \alpha < 1$  our model interpolates between the two, and for  $\alpha > 1$  the agents change their opinion with little attention to others' opinion.

We first consider a well-mixed population, that is, agents are the nodes of a complete network and therefore every agent can directly exchange votes with all the other agents. Despite being an idealised case, it allows us to build a deep analytical understanding of our model in Section III, preliminary to the study of a population interacting on a heterogeneous network in Section IV.

### III. MEAN-FIELD ANALYSIS

Let us introduce the proportion of agents with opinion  $A$  (resp.  $B$ ),  $a(t) = n_A(t)/N$  (resp.  $b(t) = n_B(t)/N$ ), hence  $a(t) + b(t) = 1$ . The proportion of agents with opinion  $A$  increases when agents with opinion  $B$  change their minds and adopt opinion  $A$ , or decreases when agents with opinion  $A$  adopt opinion  $B$ . As illustrated in Appendix A, by exploiting the well-mixed hypothesis, we obtain the time evolution of  $a(t)$  in the form of the following ordinary differential equation

$$\frac{da}{dt} = -a + P_\alpha \left( \frac{a}{a(1-Q) + Q} \right) =: f_\alpha(a). \quad (4)$$

Because the population size is finite and fixed ( $a+b=1$ ), Eq. (4) is sufficient to fully determine the temporal dynamics of the system, without the need to explicitly define another equation ruling the evolution of the proportion of agents with opinion  $B$ .

We analyse the long-term dynamics of the system by finding the equilibria of Eq. (4) and computing their stability as a function of the model parameters. The equilibria are found at values of  $a$  that satisfy  $f_\alpha(a) = 0$ . We find that  $\hat{a}^* = 1$  and  $\check{a}^* = 0$  are always two zeros of  $f_\alpha(a)$ . When these equilibria are stable, they correspond to a consensus decision for either alternative: for  $\hat{a}^* = 1$ ,

all agents eventually have opinion  $A$ , that is, the population has selected the best option (because  $Q_A > Q_B$ ), or, when  $\check{a}^* = 0$ , all agents eventually have opinion  $B$  and therefore the population has made a collective mistake by selecting the option with the inferior quality. For a range of values of  $\alpha$  and  $Q$ , a third equilibrium  $\tilde{a}^* \in (0, 1)$  may exist and it corresponds to a polarised population, in which agents with opinion  $A$  and  $B$  coexist. In this case, there is not a consensus decision but the population is in a decision deadlock. Recall that  $Q < 1$ ; therefore, we can prove (as detailed in Appendix A) that

- i) if  $Q > \alpha$ , both  $\check{a}^* = 0$  and  $\hat{a}^* = 1$  are *stable* equilibria, and a third equilibrium  $0 < \tilde{a}^* < 1$  exists and is *unstable*;
- ii) if  $Q < \alpha < 1/Q$ , then  $\check{a}^* = 0$  is *unstable* while  $\hat{a}^* = 1$  is *stable*, the third equilibrium  $0 < \tilde{a}^* < 1$  does not exist;
- iii) if  $Q < \alpha$ , both  $\check{a}^* = 0$  and  $\hat{a}^* = 1$  are *unstable* equilibria, and a third equilibrium  $0 < \tilde{a}^* < 1$  exists and is *stable*.

Note that when the third equilibrium  $\tilde{a}^*$  exists and it is unstable – i.e., the case (i) above – the fate of the system depends on the initial conditions. Stated differently, the position of the third equilibrium  $a^*$  splits the interval  $[0, 1]$  into two parts  $[0, \tilde{a}^*]$  and  $(\tilde{a}^*, 1]$ , and if the initial conditions are such that  $a(0) \in [0, \tilde{a}^*]$ , then  $a(t) \rightarrow 0$  (and thus  $b(t) \rightarrow 1$ ), while if  $a(0) \in (\tilde{a}^*, 1]$ , then  $a(t) \rightarrow 1$  (and thus  $b(t) \rightarrow 0$ ). If there are only two equilibria – i.e., the case (ii) above – the system converges to  $\hat{a}^* = 1$  for any initial conditions (which correspond to the accurate collective decision, being  $Q_A > Q_B$ ).

In Fig. 2, we show the bifurcation diagram of the mean-field model of Eq. (4) for  $Q_A = 1$  and  $Q_B = 0.9$ , as a function of  $\alpha$ . We report the equilibria and their stability (in green when stable and in red when unstable) for values of  $\alpha$  in the range  $[0, 2]$  (x-axis). Note that  $\check{a}^* = 0$  (corresponding to a population fully committed to the inferior option  $B$ ) is a stable equilibrium for  $\alpha < Q$  and unstable otherwise. Similarly,  $\hat{a}^* = 1$  (corresponding to a population fully committed to the best option  $A$ ) is a stable equilibrium for  $\alpha < 1/Q$  (that is  $1/0.9 \approx 1.11$  for the used values of  $Q_A$  and  $Q_B$ ) and unstable in the remaining range of  $\alpha$ . The third equilibrium  $0 < \tilde{a}^* < 1$ , associated with a population where opinions  $A$  and  $B$  coexist, is unstable for  $\alpha < Q$  (red branch), stable for  $\alpha > 1/Q$  (green branch), and does not exist for  $Q < \alpha < 1/Q$ .

In Fig. 2, we also overlay to the analytical bifurcation diagram the results obtained from the numerical stochastic simulation of a system defined on a complete graph made of  $N = 500$  agents, using the same values for the opinion quality,  $Q_A = 1$  and  $Q_B = 0.9$ . For each value of  $\alpha \in [0, 2]$ , we numerically integrate the system for 50 000 time-steps and report the average of the final proportion of agents with opinion  $A$  (i.e.,  $\langle n_A \rangle / N$ ) over 21 runs. When  $\alpha < Q_B$ , the mean-field theory predicts that the system converges to  $\check{a}^* = 0$  if the initial condition

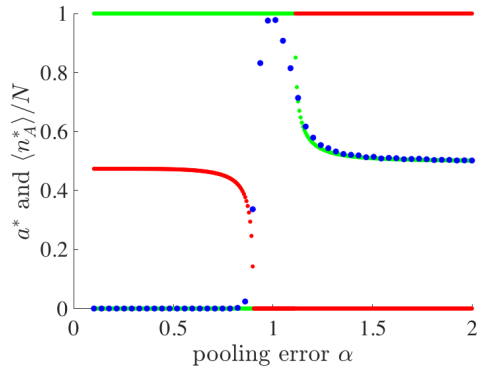


FIG. 2. Bifurcation diagrams showing the equilibria of the mean-field model of Eq. (4) as a function of  $\alpha \in [0, 2]$  for  $Q_A = 1$  and  $Q_B = 0.9$ . Green dots show stable equilibria, red dots show unstable equilibria, and blue dots show the average asymptotic values of  $\langle n_A \rangle / N$  obtained with stochastic numerical simulations of a population of  $N = 500$  agents interacting on a complete graph and initialised at  $n_A(0) = 100$ . The match between mean-field model predictions and simulations is good.

is below the value of the third unstable equilibrium  $\tilde{a}^*$ . In agreement with the theoretical predictions, our simulations, which have been initialised with  $n_A(0) = 100$  (i.e.,  $a = 0.2$ ), reached the final system state  $n_A = 0$  for  $\alpha < Q$  (blue dots in Fig. 2). When only two equilibria exist, the mean-field analysis predicts convergence to  $\hat{a}^* = 1$  for any initial conditions, and indeed the blue points (up to finite size effects) converge to  $n_A = N$ . Finally for large  $\alpha$ , when the third equilibrium is stable, according to the mean-field analysis, the system should oscillate about this third equilibrium; the numerical results agree well with the analytical predictions, with the blue dots aligned with the green curve.

Fig. 3a shows the stability diagram of the mean-field system of Eq. (4) as a function of the parameters  $\alpha$  and  $Q$ . The parameter space is divided into three regions, determined by the stability of the system equilibria. The three regions are delimited by the curves  $\alpha = Q$  (white curve) and  $\alpha = 1/Q$  (black curve), and correspond to the three stability cases described above in this section (see Appendix C for the analytical derivation of such curves). The large red region corresponds to model parameters by which the population correctly chooses the opinion with the highest quality for any initial conditions (case (ii) above, equilibrium  $\check{a}^* = 0$  is unstable and  $\hat{a}^* = 1$  is stable). In the blue region, the population remains undecided, composed of two sub-populations, each with a different opinion (case (iii) above, equilibria  $\check{a}^* = 0$  and  $\hat{a}^* = 1$  are unstable and  $0 < \check{a}^* < 1$  is stable). In the green region, the population can converge to the best or the worst option depending on the initial condition, therefore there is the possibility the population may make a collective mistake (case (i) above, equilibria  $\check{a}^* = 0$  and  $\hat{a}^* = 1$  are stable and  $0 < \check{a}^* < 1$  is unstable).

These mean-field predictions match well with the results shown in Fig. 3b, obtained from the numerical simulation of a population of  $N = 500$  agents interacting on a complete graph. The outcome of the decision is colour-coded in the RGB space, colouring each pixel with an RGB colour where the red value  $R \in [0, 1]$  corresponds to the proportion of simulations terminating with accurate decisions ( $n_A = N$ ), the green value  $G \in [0, 1]$  to the proportion of simulations terminating with incorrect decisions ( $n_A = 0$ ), and the blue value  $B \in [0, 1]$  to the proportion of simulations terminating without a consensus decision ( $0 < n_A < N$ ) after 50 000 time-steps.

Figs. 3a-b show that only when the agents have a high pooling error ( $\alpha > 1$ ), corresponding to a low cognitive load, the population can remain deadlocked at indecision. This happens in the blue region which increases in size as the cognitive load decreases (i.e., increasing pooling error  $\alpha$ ) or the decision problem difficulty increases (i.e., increasing quality ratio  $Q$ ). This is caused by agents that are rarely capable of changing their opinion based on the real distribution of opinions in the population. Interestingly, despite the poor skills of the agents, the population can either select the best option and make an accurate decision or remain undecided but it never selects the inferior option with the lower quality. Differently, decision deadlocks do not occur for any cognitive level higher or equal than the voter model, i.e.,  $\alpha \leq 1$ , however, decision mistakes can be made. For any given pooling error  $\alpha < 1$  (i.e., relatively high cognitive level), as the decision problem becomes harder (i.e., the quality ratio  $Q$  increases), the possibility of making a mistake increases. The collective mistake occurs when the system moves to a state below the unstable equilibrium,  $a < \check{a}^*$ . As shown in Figs. 4a-b, the equilibrium  $\check{a}^*$  decreases to lower values with decreasing quality ratio  $Q$ , leading to a lower rate of mistakes for easier (low  $Q$ ) problems, as visible in the green shading of Fig. 3b.

An additional result that may not be obvious is that the red region in Figs. 3a-b – which corresponds to reliably accurate decisions – is maximised for intermediate cognitive load levels (i.e.,  $\alpha = 1$  shown as a dashed horizontal grey line) and it reduces as the agent cognitive load increases. However, we can appreciate a more complete picture of the system dynamics by also analysing the decision time. Fig. 3c shows the time-steps needed to reach a consensus for a population of  $N = 500$  simulated agents interacting on a complete graph. The comparison of Figs. 3b and 3c shows the existence of a speed-accuracy trade-off, in which the speed to make a decision is traded with the collective accuracy, as it has been already documented in previous work [13, 21, 23, 45]. Therefore, increasing agents' cognitive load allows the population to quickly reach a consensus at the cost of possible decision mistakes (here shown as a wider green region in Figs. 3a-b).

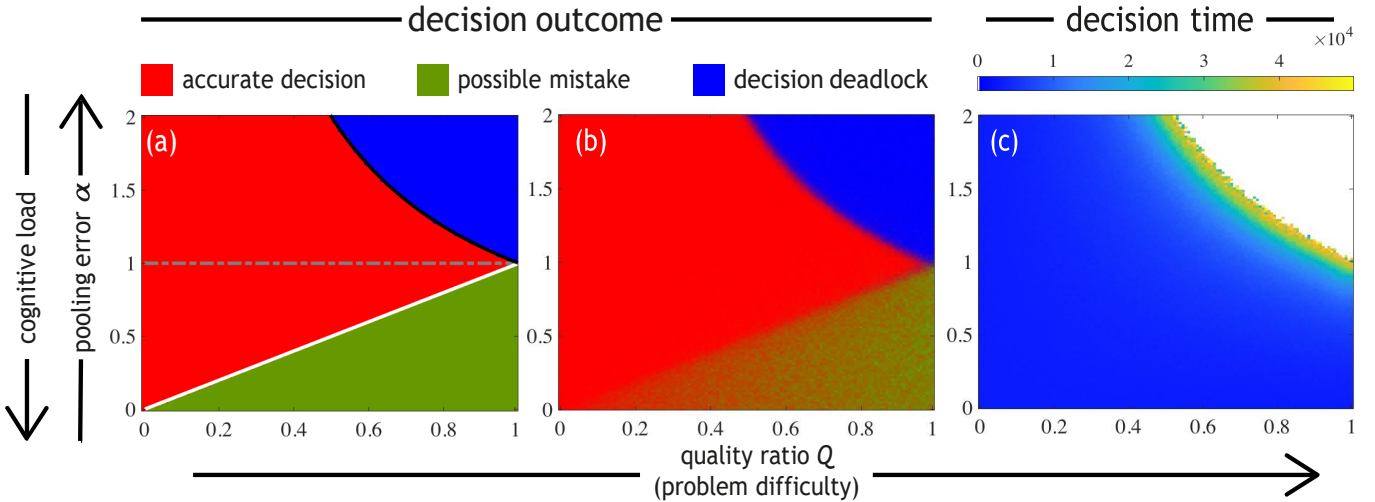


FIG. 3. Stability diagrams and convergence time. In panel (a) we report the stability diagram of the mean-field model (4) as a function of the quality ratio  $Q$  and the pooling error  $\alpha$  (inversely proportional to the cognitive cost). The parameter space is divided into three regions: in the red region the population makes accurate collective decisions for any initial condition; in the blue region the population remains locked at indecision with agents' opinions fluctuating between the two options; in the green region, a consensus for either alternative is possible depending on the initial conditions, therefore mistakes are possible. The three regions are separated by the curves  $\alpha = Q$  (white curve) and  $\alpha = 1/Q$  (black curve). Panels (b-c) show the results from simulations of  $N = 500$  agents interacting on a fully connected (all-to-all) network. For each couple  $(Q, \alpha)$ , we perform 100 independent simulations with random initial configurations (i.e. the initial number of agents with opinion  $A$  is uniformly drawn in  $[0, N]$  at each run). In (b), the RGB colour of each pixel is computed by assigning to the three values R, G, and B a value equal to the proportion of simulations that terminated at  $n_A = 500$ ,  $n_A = 0$ , and  $0 < n_A < 500$ , respectively. In (c), the colormap shows the average number of time-steps needed to reach a consensus, i.e.,  $n_A = 500$  or  $n_B = 500$ , as a function of  $Q$  and  $\alpha$ .

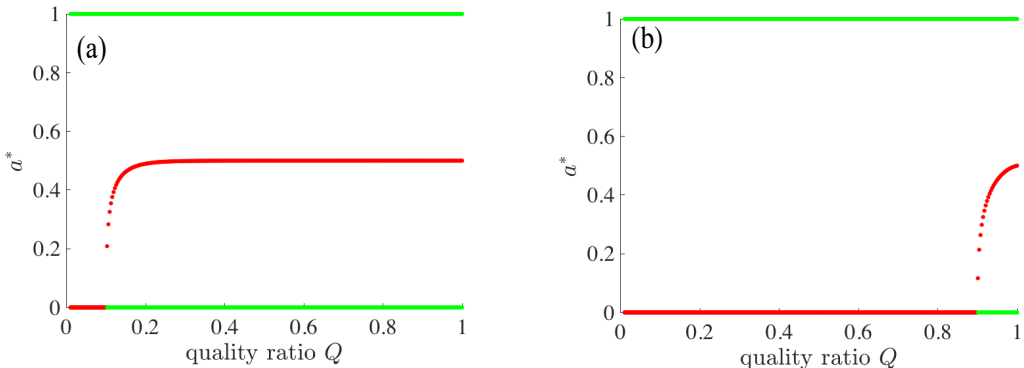


FIG. 4. Bifurcation diagrams of the mean-field model (4) as a function of the quality ratio  $Q = Q_B/Q_A$  (i.e., the problem difficulty) for fixed cognitive load,  $\alpha = 0.1$  in panel (a) and  $\alpha = 0.9$  in panel (b).

#### IV. HETEROGENEOUS MEAN-FIELD ANALYSIS

In this section, we relax the assumption of full connectivity and instead hypothesise that each agent can only exchange her opinion with a limited number of peers, i.e., with her neighbours. Thus, we can represent each agent as a node of a network connected through links to a subset of other agents from which she can receive and send information. The network of connections is described by the adjacency matrix  $\mathbf{A}$ , such that  $A_{ij} = 1$  if and only

if agents  $i$  and  $j$  are connected, and  $A_{ij} = 0$  otherwise. We also assume the network to be undirected, that is  $A_{ij} = A_{ji}$ , simple, that is at most one link can connect two nodes, and connected, that is starting from any node, there is a sequence of links that allows reaching any other node.

When agent  $i$  is selected, she pools information from her neighbours to change her opinion. Agent  $i$  has  $k_i = \sum_j A_{ij}$  neighbours, of which  $n_{i,A}$  have opinion  $A$  and  $n_{i,B}$  have opinion  $B$ , thus,  $k_i = n_{i,A} + n_{i,B}$ . The number of  $i$ 's neighbours  $k$  corresponds to the degree of the node

i. Analogous to Eq. (1), but assuming a sparse network, the votes expressed by the neighbours of  $i$  in favour of options  $A$  and  $B$  are, respectively,

$$\begin{aligned} n_{i,A}^\# &= \frac{Q_A n_{i,A}/k_i}{Q_A n_{i,A}/k_i + Q_B n_{i,B}/k_i} \quad \text{and} \\ n_{i,B}^\# &= \frac{Q_B n_{i,B}/k_i}{Q_A n_{i,A}/k_i + Q_B n_{i,B}/k_i}. \end{aligned} \quad (5)$$

As further described in Appendix B, once agent  $i$  interacts with her neighbours, she adopts opinion  $A$  or  $B$  with probability  $P_\alpha(n_{i,A}^\#)$  or  $P_\alpha(n_{i,B}^\#)$ , respectively, as we also recall that  $P_\alpha(n_{i,A}^\#) + P_\alpha(n_{i,B}^\#) = 1$ .

By assuming the Heterogeneous Mean Field hypothesis [31, 32] to be valid, we hypothesise that all nodes with the same degree exhibit the same behaviour. Therefore, we can define  $A_k$  (resp.  $B_k$ ) as the number of agents, i.e., nodes, with degree  $k$  and opinion  $A$  (resp. opinion  $B$ ), and  $N_k$  as the total number of agents with degree  $k$ . Hence,  $A_k + B_k = N_k$  for all  $k$ . In a similar way to the mean-field analysis of Sec. III, we define  $a_k = A_k/N_k$  (resp.  $b_k = B_k/N_k$ ) as the proportion of agents having opinion  $A$  (resp.  $B$ ) among all agents with degree  $k$ ; hence, for all  $k$  we have  $a_k + b_k = 1$ .

Let us now describe the time evolution of  $a_k$  for a generic  $k$ . The proportion  $a_k$  increases when an agent with degree  $k$  and opinion  $B$  changes her opinion to  $A$ , or it decreases when an agent with degree  $k$  and opinion  $A$  changes her opinion to  $B$ . To compute the frequency of these events, we compute  $n_{i,A}^\#$  and  $n_{i,B}^\#$  given in Eq. (5) under the HMF assumption. The HMF theory originated in epidemiology, which uses the concept of *excess degree* [46] to compute the infection probability of a focal agent. The excess degree is the number of neighbours that a neighbour of the focal agent has, without considering the focal agent. In other words, the excess degree of an agent is its number of neighbours minus one (see Fig. 5). We define  $p_k$  as the probability that a uniformly random chosen node has degree  $k$ , and  $q_k$  as the probability for a node to have excess degree equal to  $k$ , which we can compute as

$$q_k = \frac{(k+1)p_{k+1}}{\langle k \rangle} \quad \forall k \geq 0, \quad (6)$$

where  $\langle k \rangle = \sum_k k p_k$  is the average node degree, and trivially  $\sum_k q_k = 1$ . Let us consider a generic focal agent  $i$  (or, equivalently, focal node  $i$ ) with degree  $k$  and opinion  $B$  (see Fig. 5); let  $q_{j_1}$  be the probability that an agent  $i_1$ , connected to the focal agent  $i$ , has excess degree  $j_1 \geq 0$ . Let  $a_{j_1+1}$  be the probability that agent  $i_1$  has opinion  $A$ , and  $b_{j_1+1} = 1 - a_{j_1+1}$  the probability she has opinion  $B$ . By considering all the  $k$  agents connected with the focal agent  $i$  we can conclude that  $q_{j_1} \dots q_{j_k}$  determines the joint probability that each agent reachable from any of the  $k$  links emerging from the former agent, has excess degree  $j_1, \dots, j_k$ . We can then define  $\pi_{k,\ell}$  as the probability that  $\ell$  agents among the  $k$  ones have opinion  $B$  and thus  $k - \ell$  agents have opinion  $A$ . Therefore,

the term  $\ell$  is a linear combination of the products of  $a_{j_m+1}$  and  $(1 - a_{j_m+1})$ , with  $m = 1, \dots, k$ . Hence, we can compute the weighted proportion of agents with opinion  $A$  as  $n_{i,A}^\# = (k - \ell)/[k - \ell + Q\ell]$ , and this event happens with probability  $q_{j_1} \dots q_{j_k} \pi_{k,\ell}$ . In conclusion, agent  $i$  with opinion  $B$  can change opinion with probability  $q_{j_1} \dots q_{j_k} \pi_{k,\ell} P_\alpha((k - \ell)/[k - \ell + Q\ell])$ . See an explanatory example for  $k = 2$  in Appendix B.

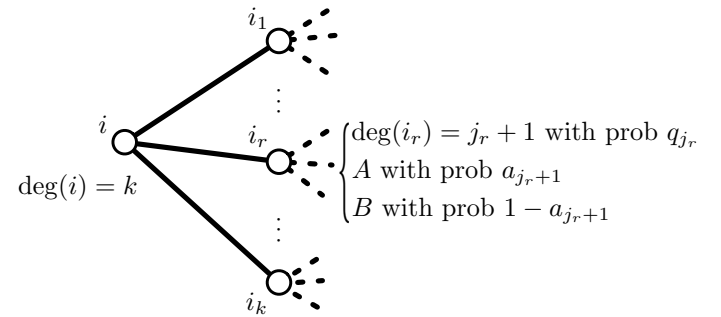


FIG. 5. Schematic representation of the probabilities involved in the heterogeneous mean-field computations. The focal node  $i$  has  $k$  neighbours (degree  $k$ ), denoted by  $i_1, \dots, i_r, \dots, i_k$ . Each neighbour, e.g., node  $i_r$ , has an excess degree  $j_r$  with probability  $q_{j_r}$  and therefore degree  $j_r + 1$ . With probability  $a_{j_r+1}$ , she has opinion  $A$ , and therefore with probability  $1 - a_{j_r+1}$ , she has opinion  $B$ .

In a similar way, we can compute the decrease rate of agents with degree  $k$  and opinion  $A$ . In this case, the argument of the function  $P_\alpha$  is  $\frac{Q_B \ell}{Q_A(k-\ell) + Q_B \ell} = \frac{Q\ell}{k-\ell+Q\ell}$ , that is, the weighted proportion of agents with opinion  $B$  assuming that  $\ell$  agents among them have opinion  $B$ . Note that, because  $P_\alpha(n_A^\#) + P_\alpha(n_B^\#) = 1$ , we have that

$$\begin{aligned} P_\alpha\left(\frac{Q\ell}{k-\ell+Q\ell}\right) &= 1 - P_\alpha\left(1 - \frac{Q\ell}{k-\ell+Q\ell}\right) \\ &= 1 - P_\alpha\left(\frac{k-\ell}{k-\ell+Q\ell}\right). \end{aligned}$$

By combining these equations and following a series of simplifications described in Appendix B, we describe the change in time of the proportion  $a_k$  as

$$\frac{da_k}{dt} = -a_k + \sum_{j_1, \dots, j_k} q_{j_1} \dots q_{j_k} \sum_{\ell=0}^k \pi_{k,\ell} P_\alpha\left(\frac{k-\ell}{k-\ell+Q\ell}\right). \quad (7)$$

To analyse the dynamics and equilibria of the system, we define

$$\langle a \rangle := \sum_{j \geq 0} q_j a_{j+1}, \quad (8)$$

and by combining it with Eq. (7), we obtain

$$\begin{aligned} \frac{d\langle a \rangle}{dt} &= -\langle a \rangle + \sum_k q_k \sum_{\ell=0}^k \binom{k+1}{\ell} \langle a \rangle^{k+1-\ell} (1 - \langle a \rangle)^\ell \times \\ &P_\alpha \left( \frac{k+1-\ell}{k+1-\ell+\ell Q} \right) := f_\alpha^{(hmf)}(\langle a \rangle). \end{aligned} \quad (9)$$

By imposing  $f_\alpha^{(hmf)}(\langle a^* \rangle) = 0$ , we can find (up to) three equilibria  $\langle a^* \rangle$ . There is the equilibrium  $\langle a^* \rangle = 0$ , where  $a_k = 0$  for all  $k$ , which corresponds to the system with no agent having opinion  $A$  (thus, all agents have opinion  $B$ ). There is the equilibrium  $\langle a^* \rangle = 1$ , where  $a_k = 1$  for all  $k$ , which corresponds to the system with all agents having opinion  $A$ . There is also a third equilibrium  $0 < \langle a^* \rangle < 1$ , which has a non-trivial mathematical expression and exists only for a certain range of parameter values. This equilibrium corresponds to the coexistence of agents with opinions  $A$  and  $B$ .

The stability of the three equilibria can be studied by analysing the sign of the derivative of  $f_\alpha^{(hmf)}$ . By following the steps described in Appendix B, the derivatives evaluated at the equilibria  $\langle a^* \rangle = 0$  and  $\langle a^* \rangle = 1$  are, respectively,

$$\begin{aligned} (f_\alpha^{(hmf)})'(0) &= -1 + \sum_k q_k (k+1) P_\alpha \left( \frac{1}{1+kQ} \right) \quad \text{and} \\ (f_\alpha^{(hmf)})'(1) &= -1 + \sum_k q_k (k+1) P_\alpha \left( \frac{Q}{k+Q} \right). \end{aligned} \quad (10)$$

Therefore, we can appreciate that the stability of both equilibria is not only determined by the parameters  $\alpha$  and  $Q$ , as in the mean-field case of Sec. III, but also by the network structure, via the probability of excess degree  $q_k$ .

### A. Scale-free networks

The heterogeneous mean-field analysis allows us to study the influence of the network topology on group dynamics. Here, we consider scale-free networks with a degree distribution that follows a power law with exponent  $\gamma > 2$ . Therefore,  $p_k = c_\gamma/k^\gamma$  (where  $c_\gamma := \left(\sum_{k \geq 1} 1/k^\gamma\right)^{-1} > 0$  is a normalising constant), the excess degree probability is  $q_k = \frac{1}{\langle k \rangle} \frac{c_\gamma}{(k+1)^{\gamma-1}}$ , and the average degree is  $\langle k \rangle = \sum_{k \geq 1} k c_\gamma/k^\gamma$ . Using the same colour code of Fig. 3a, Fig. 6 shows the stability diagrams for  $\gamma \in \{2.2, 2.6, 3.1\}$  as a function of the parameters  $\alpha$  and  $Q$ , defining the individual cognitive load and the decision-problem difficulty, respectively. We can appreciate that, as the exponent  $\gamma$  increases, the size of the red region increases and the size of the green region decreases (on the other hand, the change in the blue region is unnoticeable). While in the green region the collective decision depends on the initial system condition (thus opening

the group to possible errors), in the red region the population cannot make mistakes but only makes accurate collective decisions for any initial condition. Therefore, the results of Fig. 6 suggest that when opinions are exchanged in networks with high  $\gamma$ , the population is more accurate in collective decision-making. The same conclusion can be reached by observing the stability diagrams of Fig. 7, in which the problem difficulty is fixed (quality ratio  $Q \in \{0.5, 0.8, 0.9\}$ ) and the stability regions are computed as a function of  $\alpha$  and  $\gamma$ .

As  $\gamma$  increases, the probability of having nodes with a large degree decreases as  $1/k^\gamma$  and most of the nodes have a very low degree (one or two neighbours). Therefore, these results suggest that collective accuracy can improve as connectivity decreases, i.e., in networks that are sparse with nodes with mostly low degrees. The counter-intuitive nature of this result – groups perform better communicating on sparse networks – can be explained by complementing the analysis with the decision time. In fact, panels (c), (f), and (i) of Fig. 7 show that as the probability of having nodes with a large degree decreases (i.e., increasing  $\gamma$ ), the average decision time slightly increases. This result supports and extends beyond the case  $\alpha = 1$  the results presented in [24]. Therefore, once again, improved accuracy is coupled with slower decisions, and in this case the speed-accuracy trade-off can be regulated by both the individual cognitive load (pooling error  $\alpha$ ) and the network connectivity (exponent  $\gamma$ ).

As a cautionary note, we also want to highlight the limitations of the HMF approach. While the model predictions are confirmed by agent-based simulations on the tested scale-free networks (Figs. 6 and 7), the model is not able to predict accurately the dynamics of a population interacting on  $2m$ -regular graphs. In particular, we investigate the dynamics of nodes interacting on ring networks where all nodes are connected to their first  $m$  neighbour nodes on the “left” and  $m$  on the “right”, in such a way all nodes have the same degree  $k = 2m$ . In Appendix C, we study the heterogeneous mean-field model for the case of  $2m$ -regular ring networks and derive the equations describing the bifurcation points that determine the stability changes of the system. Fig. 8 shows stability diagrams (left column panels) for  $m \in \{2, 3, 10\}$  that are qualitatively similar to the ones computed for the other types of networks (complete graph and scale-free networks). However, the central column panels of Fig. 8 show that the results of the numerical simulations only partially agree with the theory predictions. The agreement improves as the connectivity increases ( $m = 10$ ), however, the dynamics for low values of  $m$  are different. In particular, we can appreciate that the agent-based simulations are able to make accurate decisions (red area) for a much larger range of parameters  $Q$  and  $\alpha$  than what the theory predicted. It is unclear whether the discrepancy is due to the regularity of the graph which the HMF model does not capture or to other factors (e.g., low connectivity), and it can be the focus of future research. Despite the current HMF model cannot grasp the dynamics on  $2m$ -

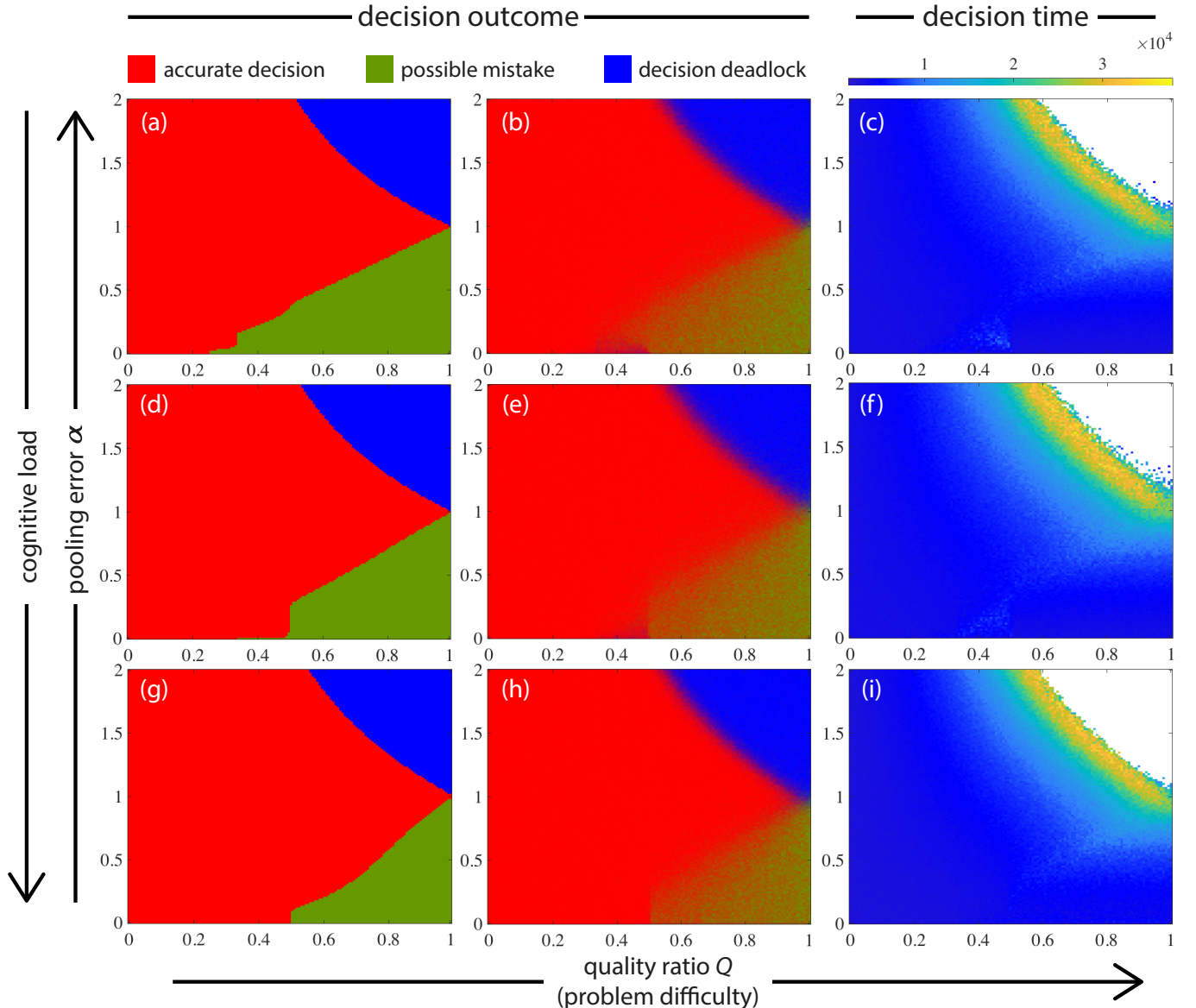


FIG. 6. Stability diagrams and convergence time for collective decision-making on scale-free networks as a function of the pooling error  $\alpha$  and quality ratio  $Q$ . We present the results for three values of the exponent  $\gamma$  regulating network connectivity: top row  $\gamma = 2.2$ , central row  $\gamma = 2.6$ , bottom row  $\gamma = 3.1$ . Left column panels – i.e., (a), (d), and (g) – show the convergence diagram of the mean-field model (9). The parameter space is divided into the same three regions of Fig. 3a using the same colour code. Central and right column panels show the results of simulations (100 independent for each  $(Q, \alpha)$  configuration) of  $N = 500$  agents interacting on a scale-free network with random initial configurations (i.e.,  $n_A(t = 0) \sim \mathcal{U}(0, N)$ ) for 50 000 time steps. Central column panels – i.e., (b), (e), and (h) – show the outcome of the collective decision-making process using the same RGB colour code as Fig. 3b. Right column panels – i.e., (c), (f), and (i) – show the average number of time-steps needed to reach a consensus, i.e.,  $n_A = 500$  or  $n_B = 500$ . The white area indicates the absence of data, as the system never reaches a consensus.

regular ring networks, the simulation results on this type of networks (Fig. 8b, e, h) confirm our intuition that collective decision-making accuracy increases as the network connectivity reduces. Population operating on networks with low  $m$  have consistently a higher accuracy. Interestingly, for  $2m$ -regular ring networks, it seems that there is no trade-off between decision speed and accuracy but, instead, rings with low  $m$  enable both quick and accurate

decisions.

## V. CONCLUSIONS

Modelling collective decision-making processes can provide useful insights into the understanding of the living world and design new decision protocols for more

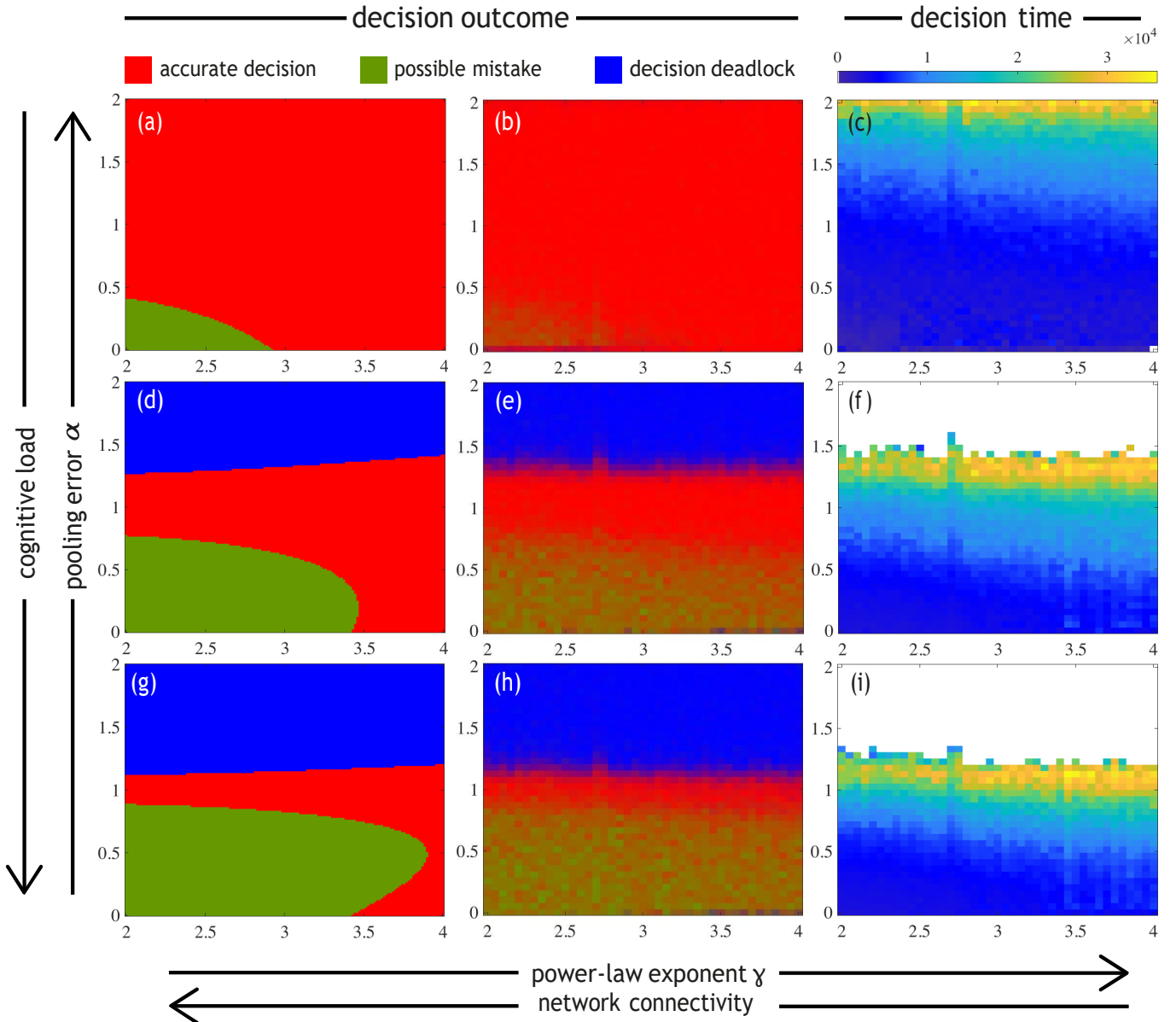


FIG. 7. Stability diagrams and convergence time for collective decision-making on scale-free networks as a function of the pooling error  $\alpha$  and network's power-law exponent  $\gamma$ . We report results for three values of the quality ratio  $Q = Q_B/Q_A$  which encodes the decision problem difficulty: top row  $Q = 0.5$  (easy problem), central row  $Q = 0.8$  (medium problem), bottom row  $Q = 0.9$  (difficult problem), with  $Q_A = 1$ . Colour code and experimental design are the same as the one described in the caption of Fig. 6.

efficient group decisions. The voter model and variations of them, thanks to their mathematical simplicity, have been effectively used to model decision-making at every level of biological complexity, from ecological dynamics of plant communities [39] to coordinated motion in fish [37] to house-hunting in honeybees [5] to human group dynamics [47, 48]. In the best-of- $n$  problem, the group has to select the best option among a discrete set of  $n$  alternatives and these models describe how opinions spread from one individual to another through voting interactions on a social network. This study presents a model capable

of generalising a set of popular existing voter-like models for collective decision-making in the best-of-2 scenario. Our analysis focuses on understanding the impact of two control parameters – the pooling error and the network connectivity – on the collective performance in terms of decision accuracy and time.

Both pooling error and the network connectivity regulate a speed-accuracy trade-off. By reducing the pooling error, and therefore demanding a higher cognitive effort from the individuals to correctly process the social information, the population can make quicker and more demo-

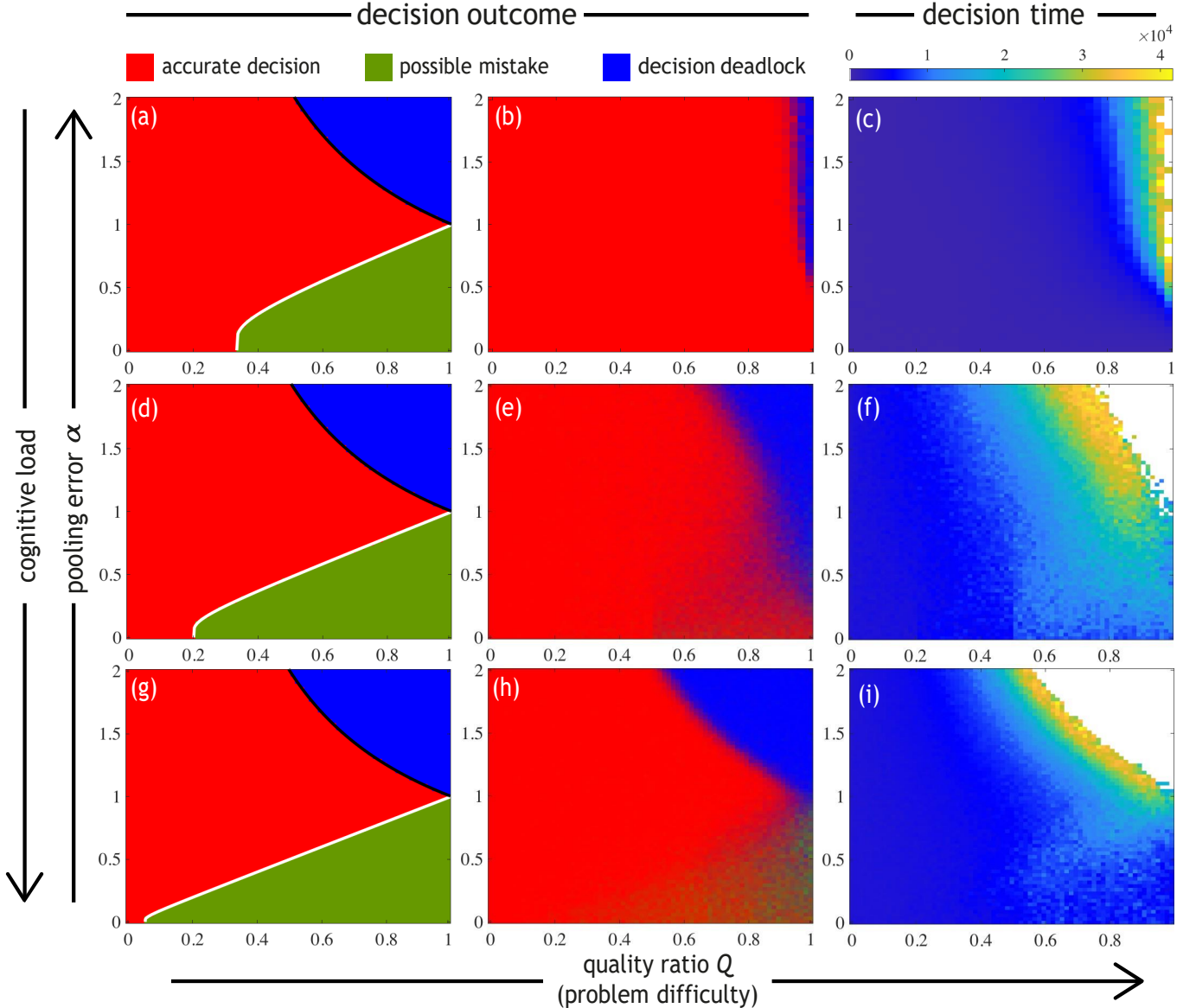


FIG. 8. Stability diagrams and convergence time for collective decision-making on  $2m$ -regular ring networks as a function of the pooling error  $\alpha$  and the quality ratio  $Q$ . We present the results for three values of the parameter  $m$  regulating network connectivity: top row  $m = 2$ , central row  $m = 3$ , bottom row  $m = 10$ . Left column panels – i.e., (a), (d), and (g) – show the convergence diagram of the HMF model (9). The parameter space is divided into the same three regions of Fig. 3a using the same colour code. Central and right column panels show the results of simulations (100 independent for each  $(Q, \alpha)$  configuration) of  $N = 500$  agents interacting on a ring network with random initial configurations (i.e.,  $n_A(t=0) \sim \mathcal{U}(0, N)$ ) for 50 000 time steps. Central column panels – i.e., (b), (e), and (h) – show the outcome of the collective decision-making process using the same RGB colour code as Fig. 3b. Right column panels – i.e., (c), (f), and (i) – show the average number of time-steps needed to reach a consensus, i.e.,  $n_A = 500$  or  $n_B = 500$ . The white area indicates the absence of data, as the system never reaches a consensus.

cratic decisions, however with reduced accuracy due to the more frequent selection of the option with the lowest quality, compared with models with higher pooling error and thus lower individual cognitive effort. Instead, by reducing network connectivity, and therefore reducing the average number of neighbours of each individual, collective accuracy is improved at the cost of higher decision time. These results improve our understanding of

the role of individual costs and network connectivity in collective decision-making.

By measuring the losses, and even the benefits, of reducing computation and communication costs, our analysis can be useful to support the design of autonomous robot systems capable of operating without human supervision. Reduced costs can save energy, money, and, in general, resources both at design and run time, i.e., de-

signing robots with simpler circuitry can be cheaper and consuming less energy in social interactions can improve efficiency. Erroneous computations and limited connectivity can not only be cheaper but also increase performance in terms of decision accuracy (due to a longer deliberation time during which the decision, rather than being rushed, is more accurately made). Recent previous results also observed that there are certain conditions where reduced connectivity between the agents of the group – robots, animals, or humans – can give important group-level advantages, e.g., better responsiveness to environmental changes [26, 28, 30], evading a predator or avoiding dangers [25, 27], or generate higher cultural diversity and innovations [49, 50]. We believe that the results of our analysis can also have important implications in the study and design of group decision-making in

human societies, which can be biased and manipulated through targeted interventions on how information is exchanged and aggregated in the social networks [51, 52].

Despite abstracting components of the process, the type of analysis proposed in our study can give useful predictions. Future work can look into extending the analysis to measure the impact of different types of network topologies, e.g., Erdős-Rényi’s random graphs, Barabási-Albert’s scale-free networks, Watts-Strogatz’s small-world network, and random geometric graphs. We also believe that an interesting extension of the work could apply the present analysis to study the dynamics of heterogeneous populations, comprising individuals that follow different voting rules or that have different levels of conformism with others (e.g., populations comprising stubborn agents [53, 54]).

---

[1] A. Reina, E. Ferrante, and G. Valentini, Collective decision-making in living and artificial systems: editorial, *Swarm Intelligence* **15**, 1 (2021).

[2] G. Valentini, E. Ferrante, and M. Dorigo, The best-of-n problem in robot swarms: Formalization, state of the art, and novel perspectives, *Frontiers in Robotics and AI* **4**, 10.3389/frobt.2017.00009 (2017).

[3] N. F. Britton, N. R. Franks, S. C. Pratt, and T. D. Seeley, Deciding on a new home: how do honeybees agree?, *Proceedings of the Royal Society of London. Series B: Biological Sciences* **269**, 1383 (2002).

[4] T. D. Seeley, P. K. Visscher, T. Schlegel, P. M. Hogan, N. R. Franks, and J. A. R. Marshall, Stop signals provide cross inhibition in collective decision-making by honeybee swarms, *Science* **335**, 108 (2012).

[5] A. Reina, J. A. R. Marshall, V. Trianni, and T. Bose, Model of the best-of-N nest-site selection process in honeybees, *Physical Review E* **95**, 052411 (2017).

[6] K. M. Passino, T. D. Seeley, and P. K. Visscher, Swarm cognition in honey bees, *Behavioral Ecology and Sociobiology* **62**, 401 (2007).

[7] G. H. Davis, M. C. Crofoot, and D. R. Farine, Using optimal foraging theory to infer how groups make collective decisions, *Trends in Ecology & Evolution* **37**, 942 (2022).

[8] L. Conradt and C. List, Group decisions in humans and animals: a survey, *Philosophical Transactions of the Royal Society B: Biological Sciences* **364**, 719 (2009).

[9] A. J. W. Ward, D. J. T. Sumpter, I. D. Couzin, P. J. B. Hart, and J. Krause, Quorum decision-making facilitates information transfer in fish shoals, *Proceedings of the National Academy of Sciences* **105**, 6948 (2008).

[10] A. Scheidler, A. Brutschy, E. Ferrante, and M. Dorigo, The k-unanimity rule for self-organized decision-making in swarms of robots, *IEEE Transactions on Cybernetics* **46**, 1175 (2016).

[11] A. Reina, R. Miletitch, M. Dorigo, and V. Trianni, A quantitative micro-macro link for collective decisions: The shortest path discovery/selection example, *Swarm Intelligence* **9**, 75 (2015).

[12] A. Reina, T. Bose, V. Trianni, and J. A. R. Marshall, Effects of spatiality on value-sensitive decisions made by robot swarms, in *Distributed Autonomous Robotic Systems (DARS 2016): The 13th International Symposium, SPAR*, Vol. 6 (Springer International Publishing, Cham, Switzerland, 2018) pp. 461–473.

[13] G. Valentini, E. Ferrante, H. Hamann, and M. Dorigo, Collective decision with 100 Kilobots: speed versus accuracy in binary discrimination problems, *Autonomous Agents and Multi-Agent Systems* **30**, 553 (2016).

[14] J. A. R. Marshall, R. Bogacz, A. Dornhaus, R. Planqué, T. Kovacs, and N. R. Franks, On optimal decision-making in brains and social insect colonies, *Journal of The Royal Society Interface* **6**, 1065 (2009).

[15] G. Valentini, H. Hamann, and M. Dorigo, Self-organized collective decision making: The weighted voter model, in *AAMAS '14: Proceedings of the 2014 international conference on Autonomous Agents and Multi-Agent Systems* (2014) pp. 45–52.

[16] V. Sood and S. Redner, Voter model on heterogeneous graphs, *Physical Review Letters* **94**, 178701 (2005).

[17] S. Redner, Reality-inspired voter models: A mini-review, *Comptes Rendus Physique* **20**, 275 (2019).

[18] P. Moretti, A. Baronchelli, M. Starnini, and R. Pastor-Satorras, Generalized voter-like models on heterogeneous networks, in *Dynamics On and Of Complex Networks, Volume 2*, Modeling and Simulation in Science, Engineering and Technology, Vol. 2 (Springer, New York, USA, 2013) pp. 285–300.

[19] A. Moinet, A. Barrat, and R. Pastor-Satorras, Generalized voterlike model on activity-driven networks with attractiveness, *Physical Review E* **98**, 022303 (2018).

[20] K. M. Passino and T. D. Seeley, Modeling and analysis of nest-site selection by honeybee swarms: the speed and accuracy trade-off, *Behavioral Ecology and Sociobiology* **59**, 427 (2006).

[21] J. A. R. Marshall, A. Dornhaus, N. R. Franks, and T. Kovacs, Noise, cost and speed-accuracy trade-offs: decision-making in a decentralized system, *Journal of The Royal Society Interface* **3**, 243 (2006).

[22] M. S. Talamali, J. A. R. Marshall, T. Bose, and A. Reina, Improving collective decision accuracy via time-varying cross-inhibition, in *Proceedings of the 2019 IEEE International Conference on Robotics and Automation (ICRA 2019)* (IEEE, 2019) pp. 9652–9659.

[23] B. C. Daniels and P. Romanczuk, Quantifying the impact of network structure on speed and accuracy in collective decision-making, *Theory in Biosciences* **140**, 379 (2021).

[24] V. Sood, T. Antal, and S. Redner, Voter models on heterogeneous networks, *Physical Review E* **77**, 041121 (2008).

[25] M. M. G. Sosna, C. R. Twomey, J. Bak-Coleman, W. Poel, B. C. Daniels, P. Romanczuk, and I. D. Couzin, Individual and collective encoding of risk in animal groups, *Proceedings of the National Academy of Sciences* **116**, 20556 (2019).

[26] D. Mateo, N. Horsevad, V. Hassani, M. Chamanbaz, and R. Bouffanais, Optimal network topology for responsive collective behavior, *Science Advances* **5**, eaau0999 (2019).

[27] P. Rahmani, F. Peruani, and P. Romanczuk, Flocking in complex environments—Attention trade-offs in collective information processing, *PLOS Computational Biology* **16**, e1007697 (2020).

[28] M. S. Talamali, A. Saha, J. A. R. Marshall, and A. Reina, When less is more: Robot swarms adapt better to changes with constrained communication, *Science Robotics* **6**, eabf1416 (2021).

[29] M. Hiraga, D. Morimoto, Y. Katada, and K. Ohkura, When less is more in embodied evolution: Robotic swarms have better evolvability with constrained communication, *Journal of Robotics and Mechatronics* **35**, 988 (2023).

[30] T. Aust, M. S. Talamali, M. Dorigo, H. Hamann, and A. Reina, The hidden benefits of limited communication and slow sensing in collective monitoring of dynamic environments, in *Swarm Intelligence (ANTS 2022)*, LNCS, Vol. 13491, edited by M. Dorigo et al. (Springer, Cham, 2022) pp. 234–247.

[31] R. Pastor-Satorras and A. Vespignani, Epidemic spreading in scale-free networks, *Physical Review Letters* **86**, 3200 (2001).

[32] V. Colizza, R. Pastor-Satorras, and A. Vespignani, Reaction–diffusion processes and metapopulation models in heterogeneous networks, *Nature Physics* **3**, 276 (2007).

[33] R. Pastor-Satorras, C. Castellano, P. Van Mieghem, and A. Vespignani, Epidemic processes in complex networks, *Reviews of modern physics* **87**, 925 (2015).

[34] G. S. Costa, M. M. de Oliveira, and S. C. Ferreira, Heterogeneous mean-field theory for two-species symbiotic processes on networks, *Physical Review E* **106**, 024302 (2022).

[35] P. Clifford and A. Sudbury, A model for spatial conflict, *Biometrika* **60**, 581 (1973).

[36] R. A. Holley and T. M. Liggett, Ergodic theorems for weakly interacting infinite systems and the voter model, *The annals of probability* **3**, 643 (1975).

[37] J. Jhawar, R. G. Morris, U. R. Amith-Kumar, M. Danny Raj, T. Rogers, H. Rajendran, and V. Guttal, Noise-induced schooling of fish, *Nature Physics* **16**, 488 (2020).

[38] J. Fernández-Gracia, K. Suchecki, J. J. Ramasco, M. San Miguel, and V. M. Eguíluz, Is the voter model a model for voters?, *Physical Review Letters* **112**, 158701 (2014).

[39] T. Zillio, I. Volkov, J. R. Banavar, S. P. Hubbell, and A. Maritan, Spatial scaling in model plant communities, *Physical Review Letters* **95**, 098101 (2005).

[40] G. De Marzo, A. Zaccaria, and C. Castellano, Emergence of polarization in a voter model with personalized information, *Physical Review Research* **2**, 043117 (2020).

[41] M. A. Montes De Oca, E. Ferrante, A. Scheidler, C. Pin- cioli, M. Birattari, M. Dorigo, M. Montes de Oca, E. Ferrante, A. Scheidler, C. Pincioli, M. Birattari, and M. Dorigo, Majority-rule opinion dynamics with differential latency: A mechanism for self-organized collective decision-making, *Swarm Intelligence* **5**, 305 (2010).

[42] P. L. Krapivsky and S. Redner, Dynamics of majority rule in two-state interacting spin systems, *Physical Review Letters* **90**, 238701 (2003).

[43] A. B. Kao and I. D. Couzin, Decision accuracy in complex environments is often maximized by small group sizes, *Proceedings of the Royal Society B: Biological Sciences* **281**, 20133305 (2014).

[44] P. Krapivsky and S. Redner, Divergence and consensus in majority rule, *Physical Review E* **103**, L060301 (2021).

[45] G. Valentini, H. Hamann, and M. Dorigo, Efficient decision-making in a self-organizing robot swarm: On the speed versus accuracy trade-off, in *Proceedings of the 14th International Conference on Autonomous Agents and Multiagent Systems*, AAMAS '15 (IFAAMAS, Richland, SC, 2015) pp. 1305–1314.

[46] M. Newman, *Networks* (Oxford University Press, New York, 2018).

[47] C. Castellano, S. Fortunato, and V. Loreto, Statistical physics of social dynamics, *Reviews of Modern Physics* **81**, 591 (2009).

[48] S. Redner, Reality-inspired voter models: A mini-review, *Comptes Rendus Physique* **20**, 275 (2019).

[49] M. Derex and R. Boyd, Partial connectivity increases cultural accumulation within groups, *Proceedings of the National Academy of Sciences* **113**, 2982 (2016).

[50] C. Gershenson and D. Helbing, When slower is faster, *Complexity* **21**, 9 (2015).

[51] I. Momennejad, Collective minds: social network topology shapes collective cognition, *Philosophical Transactions of the Royal Society B: Biological Sciences* **377**, 10.1098/rstb.2020.0315 (2022).

[52] J. B. Bak-Coleman, M. Alfano, W. Barfuss, C. T. Bergstrom, M. A. Centeno, I. D. Couzin, J. F. Donges, M. Galesic, A. S. Gersick, J. Jacquet, A. B. Kao, R. E. Moran, P. Romanczuk, D. I. Rubenstein, K. J. Tombak, J. J. Van Bavel, and E. U. Weber, Stewardship of global collective behavior, *Proceedings of the National Academy of Sciences* **118**, e2025764118 (2021).

[53] M. Mobilia, Does a single zealot affect an infinite group of voters?, *Physical Review Letters* **91**, 028701 (2003).

[54] A. Reina, R. Zakir, G. De Masi, and E. Ferrante, Cross-inhibition leads to group consensus despite the presence of strongly opinionated minorities and asocial behaviour, *Communications Physics* **6**, 236 (2023).

## Supplementary Material. Studying speed-accuracy trade-offs in best-of-n collective decision-making through heterogeneous mean-field modelling

### Appendix A: The mean-field model

In this appendix, we first indicate the steps needed to deduce the mean-field system of Eq. (4) and then we find the equilibria of the system and study their stability.

Let us introduce the proportion of agents with opinion  $A$  (resp.  $B$ ),  $a(t) = n_A(t)/N$  (resp.  $b(t) = n_B(t)/N$ ), hence  $a(t) + b(t) = 1$ . The proportion of agents with opinion  $A$  increases because agents with opinion  $B$  change their minds and adopt opinion  $A$ , or decreases if agents with opinion  $A$  adopt opinion  $B$ ; therefore, we can write the change of  $a$  in a small time interval  $dt \rightarrow 0$  as

$$\frac{da}{dt} = bP_\alpha(a^\#) - aP_\alpha(b^\#). \quad (\text{A1})$$

We recall the quantities  $n_A^\#$  and  $n_B^\#$  defined in Eq. (1), representing the votes expressed for option  $A$  and  $B$ , respectively, which are weighted by the quality. Therefore, we can define the weighted proportions

$$a^\# = \frac{a}{a + Qb} \quad \text{and} \quad b^\# = \frac{Qb}{a + Qb}, \quad (\text{A2})$$

where  $Q$  is the ratio  $Q_B/Q_A$ . Given the functional form of  $P_\alpha$  given in Eq. (2), we can conclude that

$$P_\alpha(a^\#) + P_\alpha(b^\#) = 1.$$

Hence, we can derive the mean-field model of Eq. (4) as

$$\frac{da}{dt} = (1 - a)P_\alpha(a^\#) - a(1 - P_\alpha(a^\#)) = P_\alpha\left(\frac{a}{a(1 - Q) + Q}\right) - a =: f_\alpha(a).$$

The equilibria of this system are determined by the zeros of  $f_\alpha(a)$ , namely we are looking for values  $a^* \in [0, 1]$  such that

$$f_\alpha(a^*) = 0, \quad \text{i.e.,} \quad P_\alpha\left(\frac{a^*}{a^*(1 - Q) + Q}\right) - a^* = 0. \quad (\text{A3})$$

The equilibrium stability is determined by the sign of the derivative computed on the equilibrium,  $f'(a^*)$ . To simplify the analysis, let us introduce a new variable

$$x = \frac{a}{a(1 - Q) + Q}. \quad (\text{A4})$$

Observe that  $x$  is well defined, indeed  $a(1 - Q) + Q \neq 0$  for  $a \in [0, 1]$  and moreover  $x = 0$  if  $a = 0$  and  $x = 1$  if  $a = 1$ . In conclusion, Eq. (A4) defines a bijective map from  $[0, 1]$  into  $[0, 1]$ . By inverting the relation (A4) we can write

$$a = \frac{xQ}{1 - x(1 - Q)}, \quad (\text{A5})$$

hence solving Eq. (A3) is equivalent to solve

$$P_\alpha(x^*) = \frac{x^*Q}{1 - x^*(1 - Q)}, \quad (\text{A6})$$

that is to determine the intersections between the function  $P_\alpha(x)$  and the hyperbola  $g(x) = \frac{xQ}{1 - x(1 - Q)}$ . Two solutions are trivially found:  $\check{x}^* = 0$  and  $\hat{x}^* = 1$ . However, for some choice of the parameters  $Q$  and  $\alpha$ , a third solution  $\tilde{x}^*$  can also exist.

To find the intersections between the two functions, let us define  $\Delta(x) = P_\alpha(x) - g(x)$ , and search for which values  $\Delta(x) = 0$ . As indicated above, for  $x = 0$  and  $x = 1$ , we have  $\Delta(0) = \Delta(1) = 0$ . To determine the existence of (at least) a third root let us consider the derivative of  $\Delta(x)$  at  $x = 0$  and  $x = 1$ . A straightforward computation returns

$\Delta'(0) = \alpha - Q$  and  $\Delta'(1) = \alpha - 1/Q$ . A sufficient condition to have a third solution is thus  $\Delta'(0) > 0$  and  $\Delta'(1) > 0$  or  $\Delta'(0) < 0$  and  $\Delta'(1) < 0$ . The reason is that the function  $\Delta(x)$  is continuous and if it approaches both  $x = 0$  and  $x = 1$  with increasing (or both decreasing) derivatives, it should cross (at least once) the 0 line at some point.

Let us now consider the stability of the three equilibria. The equilibrium  $\check{x}^* = 0$  is stable if and only if  $\Delta'(0) < 0$ , namely if  $\alpha < Q$ . On the other hand, the equilibrium  $\hat{x}^* = 1$  is stable if and only if  $\Delta'(1) < 0$ , namely  $\alpha < 1/Q$ . From Eq. (A5) one can obtain the value of the variable  $a$  given  $x$ , we can thus draw the following conclusions:

- Let  $Q > 1$ :

- if  $\alpha < 1/Q$ , then we also have  $\alpha < Q$ , thus  $\check{x}^* = 0$  and  $\hat{x}^* = 0$  are *stable* equilibria, and the third equilibrium  $0 < \tilde{x}^* < 1$  exists but it is *unstable*;
- if  $1/Q < \alpha < Q$ , then  $\check{x}^* = 0$  is *stable*,  $\hat{x}^* = 0$  is *unstable*, and the third equilibrium  $0 < \tilde{x}^* < 1$  does not exist;
- if  $Q < \alpha$ , then  $\check{x}^* = 0$  and  $\hat{x}^* = 0$  are *unstable* equilibria, and the third equilibrium  $0 < \tilde{x}^* < 1$  exists and is *stable*.

- Let  $Q < 1$ :

- if  $\alpha < Q$ , then we also have  $\alpha < 1/Q$ , thus  $\check{x}^* = 0$  and  $\hat{x}^* = 0$  are *stable* equilibria, and the third equilibrium  $0 < \tilde{x}^* < 1$  exists but is *unstable*;
- if  $Q < \alpha < 1/Q$ , then  $\check{x}^* = 0$  is *unstable*,  $\hat{x}^* = 0$  is *stable*, and the third equilibrium  $0 < \tilde{x}^* < 1$  does not exist;
- if  $Q < \alpha$ , then  $\check{x}^* = 0$  and  $\hat{x}^* = 0$  are *unstable* equilibria, and the third equilibrium  $0 < \tilde{x}^* < 1$  exists and is *stable*.

## Appendix B: The heterogeneous mean-field model

In this section, we present the detailed computation needed to derive through heterogeneous mean-field theory Eqs. (7) and (9), presented in the main text. Let us assume that agents are connected via a network and they can exchange opinions only with neighbours to which they are directly connected. Given an agent  $i$ , her neighbours are defined as the nodes  $j$  for which  $A_{ij} = 1$ , where  $\mathbf{A}$  is the  $N \times N$  adjacency matrix. Observe that  $A_{ij} = 0$  if agents  $i$  and  $j$  are not connected and therefore cannot directly exchange opinions.

Let us introduce the quantities  $n_{i,A}$  and  $n_{i,B}$  that indicate the number of neighbours of agent  $i$  with opinion  $A$  and  $B$ , respectively. Formally, we can define them as

$$n_{i,A} = \sum_j A_{ij} \hat{A}_j \quad \text{and} \quad n_{i,B} = \sum_j A_{ij} \hat{B}_j, \quad (\text{B1})$$

where  $\hat{A}_j = 1$  (resp.  $\hat{B}_j = 1$ ) if agent  $j$  has opinion  $A$  (resp.  $B$ ), and zero otherwise.

An agent  $i$  with opinion  $A$  (resp.  $B$ ) changes her opinion to  $B$  (resp.  $A$ ) with probability defined by the nonlinear function  $P_\alpha(n_{i,B}^\#)$  (resp.  $P_\alpha(n_{i,A}^\#)$ ) presented in Eq. (2), with argument the weighted proportion  $n_{i,B}^\#$  (resp.  $n_{i,A}^\#$ ) of  $i$ 's neighbours with opinion  $B$  (resp.  $A$ ). The weights of  $n_{i,A}^\#$  and  $n_{i,B}^\#$  are proportional to the quality of opinions  $A$  and  $B$ , respectively, and can be mathematically defined as

$$n_{i,A}^\# = \frac{Q_A n_{i,A}}{Q_A n_{i,A} + Q_B n_{i,B}} \quad \text{and} \quad n_{i,B}^\# = \frac{Q_B n_{i,B}}{Q_A n_{i,A} + Q_B n_{i,B}}. \quad (\text{B2})$$

We recall that  $k_i = \sum_j A_{ij}$  is the degree of the node  $i$  and trivially  $k_i = n_{i,A} + n_{i,B}$ . Let us observe that by defining  $Q = Q_B/Q_A$  we can rewrite the previous relations as:

$$n_{i,A}^\# = \frac{n_{i,A}}{n_{i,A} + Q n_{i,B}} = \frac{n_{i,A}}{(1 - Q) n_{i,A} + Q k_i} = \frac{n_{i,A}/k_i}{(1 - Q) n_{i,A}/k_i + Q} \quad \text{and} \quad n_{i,B}^\# = 1 - n_{i,A}^\#, \quad (\text{B3})$$

namely Eq. (5) in the main text.

Let us now assume the validity of the Heterogeneous Mean Field hypothesis (HMF) [31, 32] and let thus aggregate agents according to their opinion and degree, namely we define  $A_k$  and  $B_k$  to be the number of agents with degree  $k$  and opinion  $A$  or  $B$ , respectively. Then, setting  $N_k$  to be the number of agents with degree  $k$ , we have  $A_k + B_k = N_k$

for all  $k$ . Let us introduce  $a_k = A_k/N_k$  and  $b_k = B_k/N_k$  as the proportion of agents with degree  $k$  and opinion  $A$  or  $B$ , respectively. The goal is to express the probability of changing opinion by using the HMF.

Let us consider an agent  $i$  with opinion  $B$  and assume she has  $k$  neighbours; and we want to compute the probability that  $\ell$  neighbours have opinion  $B$  and  $k - \ell$  opinion  $A$  (with  $\ell \in \{0, \dots, k\}$ ), so that we can compute the weighted proportions of Eq. (B2) as  $n_{i,A}^\# = (k - \ell)/[k - \ell + Q\ell]$  and  $n_{i,B}^\# = \ell Q/[k - \ell + Q\ell]$ . In the spirit of the HMF hypothesis, we determine the probability that a node has degree  $k'$  by only knowing that it is connected to a node with degree  $k$ ; the latter is given by the *excess degree*  $q_{k'}$ , namely  $q_{k'} = (k' + 1)p_{k'+1}/\langle k \rangle$ , where  $p_k$  is the proportion of nodes with degree  $k$  and  $\langle k \rangle$  the average network degree.

#### Example for $k = 2$

Before computing the formula for a general degree  $k$ , let us present an example for  $k = 2$  which helps us to explain our reasoning. Assume the focal agent  $i$  has degree  $k_i = 2$  and the two neighbours have excess degree  $j_1 \geq 0$  and  $j_2 \geq 0$ , then there are three possible cases:

- Both neighbours have opinion  $A$ . This happens with probability

$$q_{j_1} a_{j_1+1} q_{j_2} a_{j_2+1},$$

- Both neighbours have opinion  $B$ . This happens with probability

$$q_{j_1} (1 - a_{j_1+1}) q_{j_2} (1 - a_{j_2+1}).$$

- One neighbour has opinion  $A$  and one neighbour has opinion  $B$ . This happens with probability

$$q_{j_1} a_{j_1+1} q_{j_2} (1 - a_{j_2+1}) + q_{j_1} (1 - a_{j_1+1}) q_{j_2} a_{j_2}.$$

Let us define  $\pi_{2,\ell}$  be the probability that  $\ell \in \{0, 1, 2\}$  agents have opinion  $B$  and thus  $2 - \ell$  opinion  $A$ . Then the previous three cases can be summarised into a single formula

$$q_{j_1} q_{j_2} \pi_{2,\ell}, \quad \forall \ell \in \{0, 1, 2\}.$$

We can now compute the probability that the focal agent  $i$  changes her opinion to  $A$ :

- In the case both neighbours have opinion  $A$ ,

$$q_{j_1} q_{j_2} \pi_{2,0} P_\alpha \left( \frac{2 - 0}{2 - 0 + 0Q} \right) = q_{j_1} q_{j_2} \pi_{2,0} P_\alpha (1).$$

- In the case both neighbours have opinion  $B$ ,

$$q_{j_1} q_{j_2} \pi_{2,2} P_\alpha \left( \frac{2 - 2}{2 - 2 + 2Q} \right) = q_{j_1} q_{j_2} \pi_{2,2} P_\alpha (0).$$

- In the case one of the two neighbours has opinion  $A$  the other has opinion  $B$ ,

$$q_{j_1} q_{j_2} \pi_{2,1} P_\alpha \left( \frac{2 - 1}{2 - 1 + 1Q} \right) = q_{j_1} q_{j_2} \pi_{2,1} P_\alpha \left( \frac{1}{1 + Q} \right).$$

#### The general case

The reasoning presented in the example for  $k = 2$  can be repeated for a general  $k$ . Then  $q_{j_1} \dots q_{j_k}$  evaluates the joint probability that each node reachable from any of the  $k$  links emerging from the focal node, has excess degree  $j_1, \dots, j_k$ . We can define  $\pi_{k,\ell}$ , to be the probability that  $\ell$  nodes among the  $k$  neighbours have opinion  $B$  and thus  $k - \ell$  opinion  $A$ . Therefore, the term  $\pi_{k,\ell}$  is a linear combination of products of  $a_{j_m+1}$  and  $(1 - a_{j_m+1})$ , with  $m = 1, \dots, k$ . Finally, the probability  $q_{j_1} \dots q_{j_k} \pi_{k,\ell}$  is multiplied by the function  $P_\alpha$  with argument the weighted proportion of agents with opinion  $A$  or  $B$ , that is  $\frac{k - \ell}{k - \ell + Q\ell}$  or  $\frac{\ell Q}{k - \ell + Q\ell}$ .

Let us observe that because of property (3) (i.e.,  $P(n_A^\#) + P(n_B^\#) = 1$ ), we have that

$$P_\alpha\left(\frac{Q\ell}{k-\ell+Q\ell}\right) = 1 - P_\alpha\left(1 - \frac{Q\ell}{k-\ell+Q\ell}\right) = 1 - P_\alpha\left(\frac{k-\ell}{k-\ell+Q\ell}\right).$$

Thus, we can wrap together the above expressions and obtain the time evolution of  $a_k$  for a generic degree  $k$ :

$$\frac{da_k}{dt} = (1-a_k) \sum_{j_1, \dots, j_k} q_{j_1} \dots q_{j_k} \sum_{\ell=0}^k \pi_{k,\ell} P_\alpha\left(\frac{k-\ell}{k-\ell+\ell Q}\right) - a_k \sum_{j_1, \dots, j_k} q_{j_1} \dots q_{j_k} \sum_{\ell=0}^k \pi_{k,\ell} \left[1 - P_\alpha\left(\frac{k-\ell}{k-\ell+\ell Q}\right)\right]. \quad (\text{B4})$$

Let us explain each term on the right-hand side. The leftmost term,  $(1-a_k)$ , is the probability that the focal agent has degree  $k$  and does not have opinion  $A$ , she hence has opinion  $B$ . The term  $q_{j_1} \dots q_{j_k}$  evaluates the joint probability that each node reachable from any of the  $k$  links emerging from the focal node, has excess degree  $j_1, \dots, j_k$ ; the sum  $\sum_{j_1, \dots, j_k}$  allows to consider all the possibilities. For a given choice of  $j_1, \dots, j_k$ , the next term,  $\pi_{k,\ell}$ , determines the probability that  $\ell$  nodes among the  $k$  ones have opinion  $B$  and thus  $k-\ell$  have opinion  $A$ . The sum  $\sum_{\ell=0}^k$  allows to consider all the possibilities from  $\ell=0$ , all agents have opinion  $A$ , to  $\ell=k$ , all agents have opinion  $B$ . Finally, the term  $P_\alpha\left(\frac{k-\ell}{k-\ell+\ell Q}\right)$  is the probability the focal agent with opinion  $B$  changes her mind because there are  $k-\ell$  agents with opinion  $A$  and  $\ell$  agents with opinion  $B$ . The remaining terms denote the opposite process where the selected agent has opinion  $A$ , with probability  $a_k$ , and she changes opinion after an interaction with her neighbours with opinion  $B$ . As already observed, we used the property (3) for the function  $P_\alpha$  to rewrite the rightmost term.

Eq. (B4) can be split into four parts

$$\begin{aligned} \frac{da_k}{dt} = & \sum_{j_1, \dots, j_k} q_{j_1} \dots q_{j_k} \sum_{\ell=0}^k \pi_{k,\ell} P_\alpha\left(\frac{k-\ell}{k-\ell+\ell Q}\right) - a_k \sum_{j_1, \dots, j_k} q_{j_1} \dots q_{j_k} \sum_{\ell=0}^k \pi_{k,\ell} P_\alpha\left(\frac{k-\ell}{k-\ell+\ell Q}\right) + \\ & - a_k \sum_{j_1, \dots, j_k} q_{j_1} \dots q_{j_k} \sum_{\ell=0}^k \pi_{k,\ell} + a_k \sum_{j_1, \dots, j_k} q_{j_1} \dots q_{j_k} \sum_{\ell=0}^k \pi_{k,\ell} P_\alpha\left(\frac{k-\ell}{k-\ell+\ell Q}\right), \end{aligned}$$

and we can observe that the rightmost terms on the first and second line do simplify each other by returning

$$\frac{da_k}{dt} = \sum_{j_1, \dots, j_k} q_{j_1} \dots q_{j_k} \sum_{\ell=0}^k \pi_{k,\ell} P_\alpha\left(\frac{k-\ell}{k-\ell+\ell Q}\right) - a_k \sum_{j_1, \dots, j_k} q_{j_1} \dots q_{j_k} \sum_{\ell=0}^k \pi_{k,\ell}. \quad (\text{B5})$$

We trivially have  $\sum_{\ell=0}^k \pi_{k,\ell} = 1$  and, by assuming absence of correlations among nodes degrees, we also have  $\sum_{j_1, \dots, j_k} q_{j_1} \dots q_{j_k} = \sum_{j_1} q_{j_1} \dots \sum_{j_k} q_{j_k} = 1$ , hence we can simplify Eq. (B5) into:

$$\frac{da_k}{dt} = \sum_{j_1, \dots, j_k} q_{j_1} \dots q_{j_k} \sum_{\ell=0}^k \pi_{k,\ell} P_\alpha\left(\frac{k-\ell}{k-\ell+\ell Q}\right) - a_k. \quad (\text{B6})$$

As already indicated in the main text, we define  $\langle a \rangle := \sum_j q_j a_{j+1}$ . By using combinatorial and assuming probability independence, we can show that

$$\sum_{j_1, \dots, j_k} q_{j_1} \dots q_{j_k} \pi_{k,\ell} = \binom{k}{\ell} \langle a \rangle^{k-\ell} (1 - \langle a \rangle)^\ell;$$

the rough idea is that in  $\pi_{k,\ell}$  there are  $k-\ell$  events with probability  $a_{j_m+1}$ , thus  $\ell$  with  $(1-a_{j_m+1})$ , and the binomial coefficient computes all possible permutations. We can thus rewrite Eq. (B6) as

$$\frac{da_k}{dt} = -a_k + \sum_{\ell=0}^{k-1} \binom{k}{\ell} \langle a \rangle^{k-\ell} (1 - \langle a \rangle)^\ell P_\alpha\left(\frac{k-\ell}{k-\ell+\ell Q}\right), \quad (\text{B7})$$

where we removed from the sum the term  $\ell=k$  because it contains  $P_\alpha(0)=0$ . By rewriting the previous equation with  $k \rightarrow k+1$ , and by multiplying both sides by  $q_k$  and summing over  $k$  to bring out  $\langle a \rangle$  we get Eq. (9) in the main

text, namely:

$$\begin{aligned} \frac{d\langle a \rangle}{dt} &= \sum_k q_k \frac{da_{k+1}}{dt} = - \sum_k q_k a_{k+1} + \sum_k q_k \sum_{\ell=0}^k \binom{k+1}{\ell} \langle a \rangle^{k+1-\ell} (1 - \langle a \rangle)^\ell P_\alpha \left( \frac{k+1-\ell}{k+1-\ell+\ell Q} \right) \\ &= -\langle a \rangle + \sum_k q_k \sum_{\ell=0}^k \binom{k+1}{\ell} \langle a \rangle^{k+1-\ell} (1 - \langle a \rangle)^\ell P_\alpha \left( \frac{k+1-\ell}{k+1-\ell+\ell Q} \right), \end{aligned}$$

where the right hand side defines the function  $f_\alpha^{(hmf)}(\langle a \rangle)$ .

#### Stability analysis

Let us now consider the zeros of  $f_\alpha^{(hmf)}(\langle a \rangle)$ , hence the equilibria of the system. Because the sum over  $\ell$  ranges from  $\ell = 0$  and  $\ell = k$ , and because the involved terms are of the form  $\langle a \rangle^{k+1-\ell}$ , they all vanish once  $\langle a \rangle = 0$ , hence  $f_\alpha^{(hmf)}(\langle a \rangle) = 0$ . The same holds true for  $\langle a \rangle = 1$ , indeed

$$f_\alpha^{(hmf)}(1) = -1 + \sum_k q_k \sum_{\ell=0}^k \binom{k+1}{\ell} (1 - \langle a^* \rangle)|_{\langle a^* \rangle=1}^\ell P_\alpha \left( \frac{k+1-\ell}{k+1-\ell+\ell Q} \right) = -1 + \sum_k q_k,$$

where we used the fact that all the terms  $(1 - \langle a^* \rangle)|_{\langle a^* \rangle=1}^\ell$  vanish except the one with  $\ell = 0$ , for which we also have  $\binom{k+1}{0} = 1$  and  $P_\alpha \left( \frac{k+1}{k+1} \right) = 1$ . The conclusion follows by recalling that  $\sum_k q_k = 1$ .

The stability of the above equilibria can be determined by considering the derivative of  $f_\alpha^{(hmf)}$  at 0 and 1 that is given by

$$\begin{aligned} \left( f_\alpha^{(hmf)} \right)'(\langle a^* \rangle) &= -1 + \sum_k q_k \sum_{\ell=0}^k \binom{k+1}{\ell} P_\alpha \left( \frac{k+1-\ell}{k+1-\ell+\ell Q} \right) \times \\ &\quad \left[ (k+1-\ell) \langle a^* \rangle^{k-\ell} (1 - \langle a^* \rangle)^\ell - \ell \langle a^* \rangle^{k+1-\ell} (1 - \langle a^* \rangle)^{\ell-1} \right], \end{aligned}$$

hence

$$\left( f_\alpha^{(hmf)} \right)'(0) = -1 + \sum_k q_k \binom{k+1}{k} P_\alpha \left( \frac{1}{1+kQ} \right) = -1 + \sum_k q_k (k+1) P_\alpha \left( \frac{1}{1+kQ} \right), \quad (\text{B8})$$

and

$$\begin{aligned} \left( f_\alpha^{(hmf)} \right)'(1) &= -1 + \sum_k q_k \left[ \binom{k+1}{0} P_\alpha \left( \frac{k+1}{k+1} \right) (k+1) - \binom{k+1}{1} P_\alpha \left( \frac{k}{k+Q} \right) \right] \\ &= -1 + \sum_k q_k (k+1) \left[ 1 - P_\alpha \left( \frac{k}{k+Q} \right) \right] = -1 + \sum_k q_k (k+1) P_\alpha \left( \frac{Q}{k+Q} \right). \quad (\text{B9}) \end{aligned}$$

In Fig. 9 we report four examples of the function  $f_\alpha(x) = x + f_\alpha^{(hmf)}(x)$  for four values of  $\alpha$  for a scale-free network with exponent  $\gamma = 2.2$ . Observe that, differently from Fig. 1, the function is smooth even for  $\alpha = 0$  (red curve). Additionally, the presence of three intersections of  $f_\alpha(x)$  with the line  $y = x$ , hence three zeros for  $f_\alpha^{(hmf)}(x)$ , indicates the presence of three system equilibria. For  $\alpha = 1$  (yellow line), there are only two line intersections, at  $x = 0$  and  $x = 1$ , indicating the existence of only two equilibria.

#### Limitations of the heterogeneous mean-field model

We conclude this appendix by studying the limitation of the heterogeneous mean-field model, more precisely we look for (family of) networks for which there is a disagreement between the dynamics predicted by the HMF model and the numerical agent-based simulations. More precisely, we look at the case in which the HMF model's equilibrium

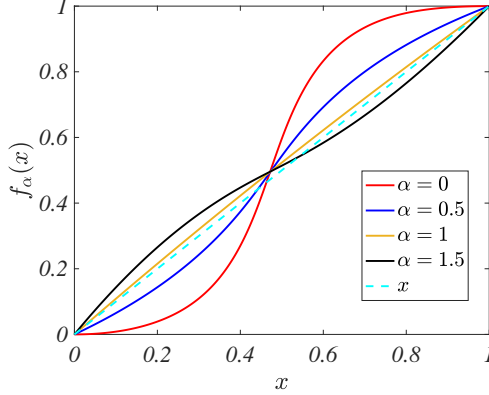


FIG. 9. The function  $f_\alpha(x) = x + f_\alpha^{(hmf)}(x)$  for some values of  $\alpha$  for a scale free network made by  $N = 400$  nodes,  $\gamma = 2.2$ ,  $k_{min} = 3$ ,  $k_{max} = 189$ , the quality ratio is  $Q = 0.9$ . The dashed line represents the identity curve and thus its intersections with the function  $f_\alpha(x)$  determine the equilibria of the system.

$\langle \check{a}^* \rangle = 0$  is unstable, i.e., Eq. (B8) is positive, and  $\langle \hat{a}^* \rangle = 1$  is stable, i.e., Eq. (B9) is negative. Therefore, the prediction is consistent convergence for any initial state to the latter stable equilibrium  $\langle \hat{a}^* \rangle = 1$ ; however, numerical simulations do not always terminate with all agents with opinion  $A$ .

For any given  $Q < 1$  there exists  $\bar{k}$  such that  $kQ > 1$  for all  $k \geq \bar{k}$  and thus  $kQ < 1$  for all  $k < \bar{k}$ . Hence

$$kQ > 1 \Rightarrow \frac{1}{1+kQ} < \frac{1}{2} \Rightarrow P_\alpha \left( \frac{1}{1+kQ} \right) = \frac{1}{2} - \frac{1}{2} \left( 1 - \frac{2}{1+kQ} \right)^\alpha,$$

and

$$kQ < 1 \Rightarrow \frac{1}{1+kQ} > \frac{1}{2} \Rightarrow P_\alpha \left( \frac{1}{1+kQ} \right) = \frac{1}{2} + \frac{1}{2} \left( \frac{2}{1+kQ} - 1 \right)^\alpha.$$

Eq. (B8) rewrites thus

$$\begin{aligned} \left( f_\alpha^{(hmf)} \right)'(0) &= -1 + \frac{1}{2} \sum_{k \geq \bar{k}} q_k(k+1) \left[ 1 - \left( 1 - \frac{2}{1+kQ} \right)^\alpha \right] + \frac{1}{2} \sum_{k < \bar{k}} q_k(k+1) \left[ 1 + \left( \frac{2}{1+kQ} - 1 \right)^\alpha \right] = \\ &= -1 + \frac{1}{2} \sum_k q_k(k+1) + \frac{1}{2} \sum_{k < \bar{k}} q_k(k+1) \left( \frac{2}{1+kQ} - 1 \right)^\alpha - \frac{1}{2} \sum_{k \geq \bar{k}} q_k(k+1) \left( 1 - \frac{2}{1+kQ} \right)^\alpha. \end{aligned}$$

By using the definition of  $q_k$ , we can compute

$$\sum_{k \geq 0} q_k(k+1) = \sum_{k \geq 0} \frac{(k+1)p_{k+1}}{\langle k \rangle} (k+1) = \frac{1}{\langle k \rangle} \sum_{k \geq 1} k^2 p_k = \frac{1}{\langle k \rangle} \sum_{k \geq 0} k^2 p_k = \frac{\langle k^2 \rangle}{\langle k \rangle},$$

hence

$$\left( f_\alpha^{(hmf)} \right)'(0) = -1 + \frac{1}{2} \frac{\langle k^2 \rangle}{\langle k \rangle} + \frac{1}{2} \sum_{k < \bar{k}} q_k(k+1) \left( \frac{2}{1+kQ} - 1 \right)^\alpha - \frac{1}{2} \sum_{k \geq \bar{k}} q_k(k+1) \left( 1 - \frac{2}{1+kQ} \right)^\alpha.$$

To compute  $\left( f_\alpha^{(hmf)} \right)'(0)$  we observe that if  $k \geq 1 > Q$  then  $Q/(k+Q) < 1/2$  and thus we can conclude

$$\begin{aligned} \left( f_\alpha^{(hmf)} \right)'(1) &= -1 + q_0 + \frac{1}{2} \sum_{k \geq 1} q_k(k+1) \left[ 1 - \left( 1 - \frac{2Q}{k+Q} \right)^\alpha \right] = \\ &= -1 + \frac{q_0}{2} + \frac{1}{2} \frac{\langle k^2 \rangle}{\langle k \rangle} - \frac{1}{2} \sum_{k \geq 1} q_k(k+1) \left( 1 - \frac{2Q}{k+Q} \right)^\alpha. \end{aligned}$$

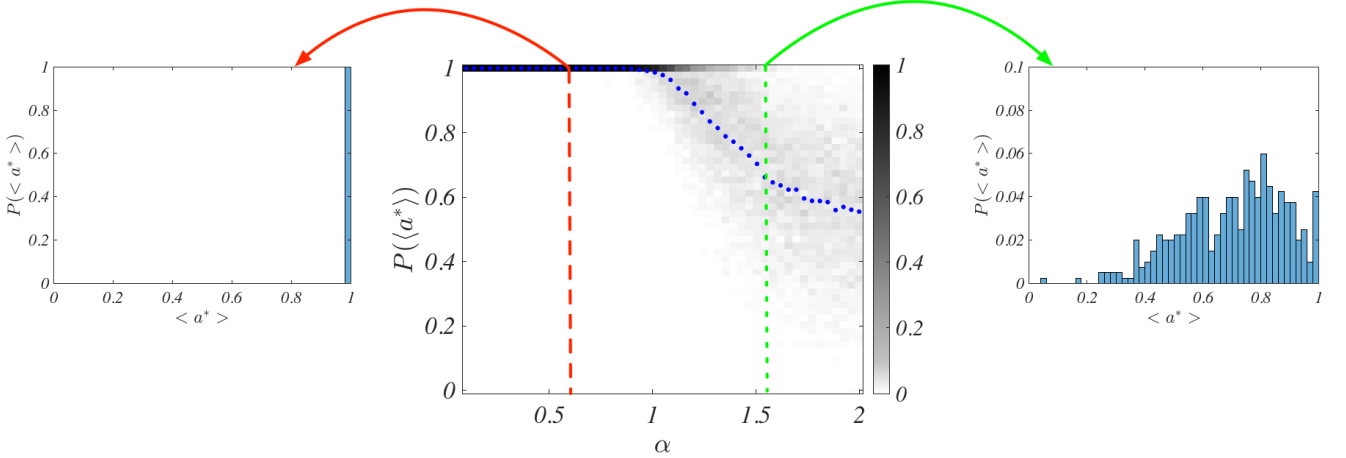


FIG. 10. Asymptotic state for the agent based model on a 2-ring. In the main panel we report the distribution of the asymptotic state  $\langle n_A^* \rangle / N$  for  $N = 500$  agents interacting in a 2-ring as a function of the parameter  $\alpha$  for a fixed  $Q = 0.9$ . For each given  $\alpha$  we repeat the simulation  $n_{iter} = 400$  times and we then we display the probability distribution of the obtained values (the darker the higher the probability). On the left panel we report the case small  $\alpha$ , here  $\alpha = 0.59$ , and we can appreciate the fact the all the simulations returned  $\langle n_A^* \rangle / N = 1$ ; on the right panel we show the case of large  $\alpha$ , here  $\alpha = 1.5$ , and we can observe a large spreading of values about the mean (blue dots in the main panel) but also the presence of a small peak corresponding to  $\langle n_A^* \rangle / N = 0$ .

For sake of definitiveness let us assume  $1/2 < Q < 1$  and thus  $\bar{k} = 2$ . Hence  $(f_\alpha^{(hmf)})'(0)$  simplifies into

$$(f_\alpha^{(hmf)})'(0) = -1 + \frac{1}{2} \frac{\langle k^2 \rangle}{\langle k \rangle} + q_1 \left( \frac{2}{1+Q} - 1 \right)^\alpha - \frac{1}{2} \sum_{k \geq 2} q_k (k+1) \left( 1 - \frac{2}{1+kQ} \right)^\alpha.$$

Finally let us consider a 2-ring network where, i.e., each node is connected with its two neighbours, hence  $\langle k \rangle = 2$ ,  $\langle k^2 \rangle = 4$ ,  $p_2 = 1$  and  $p_k = 0$  for all  $k \neq 2$  and thus  $q_1 = 1$  and  $q_k = 0$  if  $k \neq 1$ . The previous equation simplifies to give

$$(f_\alpha^{(hmf)})'(0) = -1 + \frac{1}{2} \frac{4}{2} + \left( \frac{2}{1+Q} - 1 \right)^\alpha = \left( \frac{2}{1+Q} - 1 \right)^\alpha > 0,$$

namely  $\langle \tilde{a}^* \rangle = 0$  is unstable under the assumption of HMF. Similarly the equation for  $(f_\alpha^{(hmf)})'(1)$  rewrites

$$(f_\alpha^{(hmf)})'(1) = -1 + \frac{1}{2} \frac{4}{2} - \frac{1}{2} q_1 2 \left( 1 - \frac{2Q}{1+Q} \right)^\alpha = - \left( \frac{1-Q}{1+Q} \right)^\alpha < 0,$$

namely  $\langle \hat{a}^* \rangle = 1$  is stable according to the HMF theory.

In Fig. 10 we show the results of numerical simulation of 500 agents exchanging opinions on a 2-ring, i.e., each agent has two neighbours. Each point is asymptotic value after 500 000 time steps, of  $\langle n_A^* \rangle / N$  averaged over 401 independent simulations as a function of  $\alpha$  for  $Q = 0.9$ . Simulations have different initial conditions (initial opinions distributed differently on the network) but always with 250 agents with opinion  $A$  and 250 agents with opinion  $B$ , i.e., half of the population committed to each option. One can observe that for  $\alpha < 1$  the simulations converge to  $\langle n_A^* \rangle / N = 1$  and thus the claim of the predictions of the HMF model are confirmed. Whereas the good match between theory and simulations is no longer valid for  $\alpha > 1$ . Theory predicts a single stable equilibria for full consensus for  $A$ , while the simulated system remains locked at indecision at  $0 < \tilde{a}^* < 1$  with only a part of the agents with opinion  $A$  and the rest with opinion  $B$ .

The different behaviour for  $\alpha > 1$  is due to finite-size effects and can be explained as follows. Let us assume to have a ring with  $N$  agents and assume that all agents but one have opinion  $A$ , we are interested in the possibility that also this last  $B$ -agent changes her mind and becomes  $A$ -agent, in this way the system reaches the equilibrium  $\langle n_A^* \rangle / N = 1$ , i.e., all  $A$ . This process should be compared with the one where one agent  $A$  becomes a  $B$ -agent, the ratio of the probabilities of those two events determines the stability (or not) of the state all  $A$ .

The probability that the event  $B \rightarrow A$  happens is the combination of the probability of selecting the  $B$ -agent, hence probability  $1/N$ , and the probability that she will receive a message from a neighbour committed to  $A$ . Because there is only one  $B$ -agent, her two neighbours have opinion  $A$  and thus  $P_\alpha(1) = 1$ . In summary,  $P(B \rightarrow A) = 1/N$ .

The probability that the event  $A \rightarrow B$  happens is the combination of the probability of selecting one of the two agents  $A$  sitting in the ring next to the unique agent  $B$ , hence probability  $2/N$ , and the probability that the selected agent  $A$  will select the message from the  $B$ -agent. The weighted proportion of agents  $B$  that are neighbours of the selected agent  $A$  is  $P_\alpha\left(\frac{Q}{1+Q}\right)$ . Being  $Q \in [0, 1]$ , the quantity  $\frac{Q}{1+Q}$  is smaller than  $1/2$  and thus  $P_\alpha\left(\frac{Q}{1+Q}\right) = \frac{1}{2} - \frac{1}{2}\left(\frac{1-Q}{1+Q}\right)^\alpha$ . In summary,  $P(A \rightarrow B) = \frac{2}{N} \left[ \frac{1}{2} - \frac{1}{2}\left(\frac{1-Q}{1+Q}\right)^\alpha \right]$ .

Finally, we can compute the ratio of the probabilities for the two events

$$\frac{P(A \rightarrow B)}{P(B \rightarrow A)} = 1 - \left(\frac{1-Q}{1+Q}\right)^\alpha.$$

Because  $\frac{1-Q}{1+Q} < 1$ , we can conclude that if  $\alpha < 1$ , then  $\frac{P(A \rightarrow B)}{P(B \rightarrow A)}$  is small and thus the system has a large probability to evolve toward a consensus for  $A$ , the event  $B \rightarrow A$  is much more probable than  $A \rightarrow B$ . On the other hand, if  $\alpha > 1$ , then the above probability approaches 1 and thus both events are (almost) equally probable. Therefore, despite the equilibrium of a consensus for  $A$  being stable, it is difficult to reach it because the two events ( $A \rightarrow B$  and  $B \rightarrow A$ ) are equally likely to happen and the system can fluctuate indefinitely.

### Appendix C: The $2m$ -regular graph

Let us consider now  $2m$ -regular graphs,  $m \geq 1$ , namely networks where all the nodes have the same degree  $2m$ . Observe that 1-dimensional rings where each node is connected to  $m$  left and  $m$  right neighbours fall in this class, that however contains more general structures. By construction we trivially have  $p_k = 1$  if  $k = 2m$  and  $p_k = 0$  otherwise, then  $\langle k \rangle = 2m$ , which implies that  $q_k = 1$  if  $k = 2m - 1$  and 0 otherwise, indeed

$$q_k = \frac{k+1}{\langle k \rangle} p_{k+1} = \begin{cases} \frac{(2m-1)+1}{2m} p_{2m} = 1 & \text{if } k+1 = 2m \\ 0 & \text{if } k+1 \neq 2m. \end{cases}$$

Therefore, the weighted average proportion of agents with opinion  $A$  simply becomes  $\langle a \rangle = a_{2m}$ . From the definition (9), we can simplify the function  $f_\alpha^{(hmf)}(x)$  and obtain

$$f_\alpha^{(hmf)}(x) = -x + \sum_{\ell=0}^{2m-1} \binom{2m}{\ell} x^{2m-\ell} (1-x)^\ell P_\alpha\left(\frac{2m-\ell}{2m-\ell+\ell Q}\right). \quad (\text{C1})$$

The derivatives of (C1) evaluated at  $\check{x}^* = 0$  and  $\hat{x}^* = 1$  are given by (see also (B8) and (B9)):

$$(f_\alpha^{(hmf)})'(0) = -1 + 2mP_\alpha\left(\frac{1}{1+(2m-1)Q}\right) \quad \text{and} \quad (f_\alpha^{(hmf)})'(1) = -1 + 2mP_\alpha\left(\frac{Q}{2m-1+Q}\right).$$

In conclusion, the equilibrium  $\check{a}_{2m}^* = 0$ , i.e., all agents have opinion  $B$ , is stable if and only if

$$(f_\alpha^{(hmf)})'(0) = -1 + 2mP_\alpha\left(\frac{1}{1+(2m-1)Q}\right) < 0,$$

and similarly  $\hat{a}_{2m}^* = 1$ , i.e., all agents have opinion  $A$ , is stable if and only if

$$(f_\alpha^{(hmf)})'(1) = -1 + 2mP_\alpha\left(\frac{Q}{2m-1+Q}\right) < 0.$$

When  $Q < 1/(2m-1)$ , then  $1/[(2m-1)Q+1] > 1/2$ , therefore, using the definition of  $P_\alpha$  we get:

$$(f_\alpha^{(hmf)})'(0) = -1 + 2m \left[ \frac{1}{2} + \frac{1}{2} \left( \frac{2}{1+(2m-1)Q} - 1 \right)^\alpha \right] = -1 + m \left[ 1 + \left( \frac{2}{1+(2m-1)Q} - 1 \right)^\alpha \right] \geq -1 + m,$$

and because  $m \geq 2$ , the latter expression is positive for all  $\alpha \geq 0$ . In conclusion, the equilibrium  $\check{a}_{2m}^* = 0$  is unstable for all  $\alpha \geq 0$  and  $Q < 1/(2m-1)$ .

Let us now consider the case  $Q > 1/(2m - 1)$ . By definition of  $P_\alpha$  we get

$$(f_\alpha^{(hmf)})'(0) = -1 + 2m \left[ \frac{1}{2} - \frac{1}{2} \left( 1 - \frac{2}{1 + (2m - 1)Q} \right)^\alpha \right] = -1 + m \left[ 1 - \left( 1 - \frac{2}{1 + (2m - 1)Q} \right)^\alpha \right],$$

and now the quantity on the right-hand side can have both signs. Let us define  $\hat{\alpha}(Q)$  as the value of  $\alpha$  for which the right-hand side vanishes for a fixed  $Q > 1/(2m - 1)$ , then we can straightforwardly obtain

$$\hat{\alpha}(Q) = \frac{\log \left( 1 - \frac{1}{m} \right)}{\log \left( 1 - \frac{2}{1 + (2m - 1)Q} \right)}. \quad (\text{C2})$$

By looking at its definition we can conclude that  $\hat{\alpha}(1) = 1$  and that  $\hat{\alpha}(Q) \rightarrow 0$  for  $Q \rightarrow 1/(2m - 1)$  (from values larger than  $1/(2m - 1)$ ). Given  $Q > 1/(2m - 1)$ , then  $(f_\alpha^{(hmf)})'(0) > 0$  for all  $\alpha > \hat{\alpha}(Q)$ ; this means that the equilibrium  $\check{a}_{2m}^* = 0$  is unstable. The function  $\hat{\alpha}(Q)$  is drawn in white in Fig. 8 and it delimits the red region where  $(f_\alpha^{(hmf)})'(0) > 0$  ( $\check{a}_{2m}^* = 0$  is unstable) and the green region where  $(f_\alpha^{(hmf)})'(0) < 0$  ( $\check{a}_{2m}^* = 0$  is stable).

Let us now consider the stability of the equilibrium  $\hat{a}_{2m}^* = 1$ . Because  $m \geq 1$  and  $Q < 1$ , we always have  $Q/(2m - 1 + Q) < 1/2$ , hence by definition of  $P_\alpha$  we obtain

$$(f_\alpha^{(hmf)})'(1) = -1 + 2m \left[ \frac{1}{2} - \frac{1}{2} \left( 1 - \frac{2Q}{2m - 1 + Q} \right)^\alpha \right] = -1 + m \left[ 1 - \left( 1 - \frac{2Q}{2m - 1 + Q} \right)^\alpha \right]. \quad (\text{C3})$$

Eq. (C3) can also have either positive and negative values. Let  $\tilde{\alpha}(Q)$  the value of  $\alpha$  for which the right-hand side of Eq. (C3) vanishes for a fixed  $Q$ , then

$$\tilde{\alpha}(Q) = \frac{\log \left( 1 - \frac{1}{m} \right)}{\log \left( 1 - \frac{2Q}{2m - 1 + Q} \right)}. \quad (\text{C4})$$

We have  $\tilde{\alpha}(1) = 1$  and  $\tilde{\alpha}(Q) \rightarrow \infty$  if  $Q \rightarrow 0^+$ . The function  $\tilde{\alpha}(Q)$  is drawn in black in Fig. 8 and it delimits the red region where  $(f_\alpha^{(hmf)})'(1) < 0$  ( $\hat{a}_{2m}^* = 1$  is stable) and the blue region where  $(f_\alpha^{(hmf)})'(1) > 0$  ( $\hat{a}_{2m}^* = 1$  is unstable).

#### Generalise to complete graphs

Let us conclude this part by showing the previous analysis returns the results obtained by using the mean-field hypothesis once we assume the underlying network to be a complete graph. To simplify the setting we will assume the network to be composed of  $N = 2N' + 1$  nodes and  $m = N'$ , hence each node has  $2N'$  neighbours. Let us observe that one trivially has  $p_k = 1$  if  $k = N - 1 = 2N'$  and  $p_k = 0$  otherwise, and  $\langle k \rangle = N - 1 = 2N'$ , which implies that  $q_k = 1$  if  $k = N - 2 = 2N' - 2 = 2(m - 1)$  and 0 otherwise. From Eq. (8) we can obtain  $\langle a \rangle = a_{N-1} = n_A/N$ , namely there is only one variable that is the proportion of agents with opinion  $A$ . From the Eq. (C1) we can get

$$f_\alpha^{(hmf)}(a_{N-1}) = -a_{N-1} + \sum_{\ell=0}^{2N'} \binom{2N'}{\ell} (a_{N-1})^{2N'-\ell} (1 - a_{N-1})^\ell P_\alpha \left( \frac{n_A}{n_A + n_B Q} \right),$$

where we recall that  $\ell = n_B$ , to be the number of agents with opinion  $B$ , and  $2N' - \ell = n_A$ , the number of agents with opinion  $A$ . Let us observe that we also added the term  $\ell = 2N'$  in the sum, whose contribution vanishes because  $P_\alpha$  does. By using  $n_A + n_B = N$  we can rewrite the previous equation as

$$\begin{aligned} f_\alpha^{(hmf)}(a_{N-1}) &= -a_{N-1} + \sum_{\ell=0}^{2N'} \binom{2N'}{\ell} (a_{N-1})^{2N'-\ell} (1 - a_{N-1})^\ell P_\alpha \left( \frac{n_A}{n_A(1 - Q) + NQ} \right) \\ &= -a_{N-1} + \sum_{\ell=0}^{2N'} \binom{2N'}{\ell} (a_{N-1})^{2N'-\ell} (1 - a_{N-1})^\ell P_\alpha \left( \frac{a_{N-1}}{a_{N-1}(1 - Q) + Q} \right), \end{aligned}$$

where in the last step we divided by  $N$  the number of agents to obtain the proportion. Being the term involving  $P_\alpha$  independent from  $\ell$ , we eventually obtain

$$\begin{aligned} f_\alpha^{(hmf)}(a_{N-1}) &= -a_{N-1} + P_\alpha \left( \frac{a_{N-1}}{a_{N-1}(1 - Q) + Q} \right) \sum_{\ell=0}^{2N'} \binom{2N'}{\ell} (a_{N-1})^{2N'-\ell} (1 - a_{N-1})^\ell = \\ &= -a_{N-1} + P_\alpha \left( \frac{a_{N-1}}{a_{N-1}(1 - Q) + Q} \right), \end{aligned}$$

where the Newton property for the binomial has been used to eventually get the same function we obtained under the mean field assumption (4).

Let us now rewrite  $\hat{\alpha}(Q)$  given by Eq. (C2) under the above assumption of complete graph, namely

$$\hat{\alpha}(Q) = \frac{\log\left(1 - \frac{1}{N'}\right)}{\log\left(1 - \frac{2}{1 + (2N' - 1)Q}\right)},$$

then letting the number of nodes to be very large,  $N = 2N' + 1 \rightarrow \infty$ , then we obtain

$$\hat{\alpha}(Q) \sim Q + \dots,$$

namely the curve separating the convergence to a consensus for option  $A$  (red region in Fig. 8) to the region where mistakes are possible (green region in Fig. 8) converges to the line  $\hat{\alpha}(Q) = Q$  in the limit of infinitely many agents, in agreement with the results reported in Fig. 3.